Received: 3 January 2022 | Revised: 23 June 2022 | Accepted: 15 September 2022

DOI: 10.1002/cac2.12364

CANCER COMMUNICATIONS Open Access

ORIGINAL ARTICLE

Activation of Piezo1 contributes to matrix stiffness-induced angiogenesis in hepatocellular carcinoma

Miao Li[1] | **Xi Zhang**[1] | **Mimi Wang**[1] | **Yaohui Wang**[2] | **Jiali Qian**[3] | **Xiaoxia Xing**[1] | **Zhiming Wang**[4] | **Yang You**[4] | **Kun Guo**[1] | **Jie Chen**[1] | **Dongmei Gao**[1] | **Yan Zhao**[1] | **Lan Zhang**[1] | **Rongxin Chen**[1] | **Jiefeng Cui**[1] | **Zhenggang Ren**[1]

[1]Liver Cancer Institute, Zhongshan Hospital, Fudan University & Key Laboratory of Carcinogenesis and Cancer Invasion, Ministry of Education, Shanghai 200032, P. R. China

[2]Department of Radiology, Shanghai Cancer Center, Fudan University, Shanghai 200032, P. R. China

[3]Department of Endocrinology, Huashan Hospital, Fudan University, Shanghai 200032, P. R. China

[4]Department of Oncology, Zhongshan Hospital, Fudan University, Shanghai 200032, P. R. China

Correspondence
Zhenggang Ren and Jiefeng Cui.
Zhenggang Ren, Liver Cancer Institute, Zhongshan Hospital, Fudan University & Key Laboratory of Carcinogenesis and Cancer Invasion, Ministry of Education, Shanghai 200032, P. R. China.
E-mail: ren.zhenggang@zs-hospital.sh.cn; cui.jiefeng@zs-hospital.sh.cn

Miao Li and Xi Zhang contributed to this study equally.

Funding information
National Natural Science Foundation of China, Grant/Award Number: 81972910

Abstract

Background: Despite integrin being highlighted as a stiffness-sensor molecule in matrix stiffness-driven angiogenesis, other stiffness-sensor molecules and their mechanosensory pathways related to angiogenesis in hepatocellular carcinoma (HCC) remain obscure. Here, we explored the interplay between Piezo1 and integrin β1 in the mechanosensory pathway and their effects on HCC angiogenesis to better understand matrix stiffness-induced angiogenesis.

Methods: The role of Piezo1 in matrix stiffness-induced angiogenesis was investigated using orthotopic liver cancer SD rat models with high liver stiffness background, and its clinical significance was evaluated in human HCC tissues. Matrix stiffness-mediated Piezo1 upregulation and activation were assayed using an in vitro fibronectin (FN)-coated cell culture system with different stiffness, Western blotting and Ca^{2+} probe. The effects of shPiezo1-conditioned medium (CM) on angiogenesis were examined by tube formation assay, wound

Abbreviations: AFP, Alpha-Fetoprotein; Ang, Angiopoietins; CCl_4, Carbon tetrachloride; CM, Conditioned Medium; COL, Collagen; CPA, collagen proportional area; CXCL16, CXC Chemokine Ligand 16; Co-IP, Co-Immunoprecipitation; EMT, Epithelial-Mesenchymal Transition; FGF, Fibroblast Growth Factor; FN, Fibronectin; HCC, Hepatocellular Carcinoma; H&E, Hematoxylin-Eosin; HIF-1α, Hypoxia-Inducible Factor 1α; HUVEC, Human Umbilical Vein Endothelial Cell; IGFBP, Insulin-like Growth Factor Binding Protein; IHC, Immunohistochemistry; LOX, Lysyl Oxidase; MVD, Microvascular Density; OS, Overall Survival; PDGF, Platelet-Derived Growth Factor; qRT-PCR, quantitative Real-Time Polymerase Chain Reaction; SDS-PAGE, Sodium Dodecyl Sulfate Polyacrylamide Gel Electrophoresis; SEM, Scanning Electron Microscopy; TB, Total Bilirubin; TCGA, the Cancer Genome Atlas; TNM, Tumor Node Metastasis; UB, Ubiquitin; UPA, Urokinase-type Plasminogen Activator; VEGF, Vascular Endothelial Growth Factor; VEGFR2, Vascular Endothelial Growth Factor Receptor 2; VHL, von Hippel-Lindau.

healing assay and angiogenesis array. The underlying mechanism by which Piezo1 participated in matrix stiffness-induced angiogenesis was analyzed by microRNA quantitative real-time polymerase chain reaction (qRT-PCR), matrix stiffness measurement, dual-luciferase reporter assay, ubiquitination assay and co-immunoprecipitation.

Results: Increased matrix stiffness significantly upregulated Piezo1 expression at both cellular and tissue levels, and high expression of Piezo1 indicated an unfavorable prognosis. High matrix stiffness also noticeably enhanced the activation level of Piezo1, similar to its expression level. Piezo1 knockdown significantly suppressed tumor growth, angiogenesis, and lung metastasis of HCC rat models with high liver stiffness background. shPiezo1-CM from HCC cells attenuated tube formation and migration abilities of vascular endothelial cells remarkably, and analysis of differentially expressed pro-angiogenic factors revealed that Piezo1 promoted the expression and secretion of vascular endothelial growth factor (VEGF), CXC chemokine ligand 16 (CXCL16) and insulin-like growth factor binding protein 2 (IGFBP2). Matrix stiffness-caused Piezo1 upregulation/activation restrained hypoxia inducible factor-1α (HIF-1α) ubiquitination, subsequently enhanced the expression of downstream pro-angiogenic factors to accelerate HCC angiogenesis. Besides, collagen 1 (COL1)-reinforced tissue stiffening resulted in more expression of Piezo1 via miR-625-5p.

Conclusions: This study unravels a new mechanism by which the integrin β1/Piezo1 activation/Ca^{2+} influx/HIF-1α ubiquitination/VEGF, CXCL16 and IGFBP2 pathway participates in matrix stiffness-driven HCC angiogenesis. Simultaneously, a positive feedback regulation loop as stiff matrix/integrin β1/miR-625-5p/Piezo1 and COL1/stiffer matrix mediates matrix stiffness-caused Piezo1 upregulation.

KEYWORDS
hepatocellular carcinoma, matrix stiffness, angiogenesis, Piezo1, HIF-1α ubiquitination

1 | BACKGROUND

Metastasis is considered a major obstacle in clinical practice to improve the therapeutic effect and prognosis of tumors. Angiogenesis is the basis of tumor growth, invasion, and metastasis [1–4]. Currently, anti-angiogenic monotherapy or combination therapy with immune checkpoint inhibitors has become an effective anti-tumor strategy [5–9]. However, only a part of tumor patients are sensitive to anti-angiogenic drugs alone, such as sorafenib, regorafenib, lenvatinib, and bevacizumab [10, 11], and many initially responsive patients easily develop resistance to drugs after a period of treatment [11, 12], implying that the mechanism of tumor angiogenesis is far from fully understood. Solid tumors generally have a strong ability to induce neovascularization which offers more nutrients and oxygen to feed tumor tissue and helps it to metastasize. Angiogenesis in healthy tissue is tightly controlled by the balance between pro-angiogenic and anti-angiogenic factors, but in tumor tissues, this balance is usually destroyed, and the angiogenic switch is almost always activated, thus making tumor tissues possess a hypervascularity phenotype [5, 10]. Besides that, microvasculature within tumor also exhibits the morphological characteristics of hyperpermeable, tortuous, and deformed [13]. These abnormal vasculature structural features remarkably heighten the invasion and metastasis phenotype of solid tumors, also attenuate the ability of chemotherapeutic drugs being delivered into tumors [1, 11], which underlines the significance of angiogenesis in tumor progression and the value of its targeted intervention. The contribution of biochemical cues within the microenvironment to tumor angiogenesis has been well researched during the last several decades [1, 14]. Many

pro-angiogenic and anti-angiogenic factors, including vascular endothelial growth factor (VEGF), fibroblast growth factor (FGF), angiopoietins (Ang), platelet-derived growth factor (PDGF), angiostatin, endostatin, thrombospondin-1, vascular endothelial growth factor receptor (VEGFR), neuropilin, and endoglin (CD105), are validated to participate in the modulation of tumor angiogenesis [2, 14, 15]. Hypoxia and inflammation, the two most common characteristics of the tumor microenvironment, are also found to augment the expression and release of pro-angiogenic factors and trigger tumor angiogenesis [15, 16]. However, the effects of biomechanical cues within the microenvironment, particularly matrix stiffness, on tumor angiogenesis remain largely uncharacterized.

Matrix stiffening and hypervascularity almost co-occur in all patients with advanced HCC and are associated with poor prognoses [10, 17]. The existing in vivo and in vitro evidence from our and other studies all supports that increased matrix stiffness strengthens the malignant characteristics of HCC cells and promotes their invasion and metastasis in different ways, including triggering epithelial-mesenchymal transition (EMT) occurrence [18, 19], facilitating pre-metastatic niche formation [20, 21], enhancing stemness characteristics [22, 23], upregulating invasion/metastasis-associated gene expression [24, 25], influencing glucose and lipid metabolic reprogramming [26, 27] and attenuating chemotherapeutic effect [18, 28-30]. Nevertheless, there are few literature about the linkage between matrix stiffness and angiogenesis in HCC. We previously uncovered an important role of stiffness mechanical signaling in driving HCC angiogenesis by increasing both VEGFR2 expression in human umbilical vein endothelial cells (HUVECs) and VEGF expression in HCC cells [31, 32]. Simultaneously, integrin-based mechanosensory pathways were confirmed to be responsible for HCC angiogenesis and other pathological changes [18, 31, 33]. Yet, little is known about whether there exist other stiffness-sensor molecules or mechanosensory pathways in matrix stiffness-induced angiogenesis.

The discovery of the Piezo1-dependent mechanosensitive pathway [34] makes the theory of integrin-based mechanosensory pathway face new challenges. As a new mechanosensitive ion channel protein, Piezo1 can convert physical stimuli into electrical and chemical signals by accelerating Ca^{2+} influx and regulate various physiological and pathological processes [34–37]. It was found that Piezo1 sensed mechanical signals and contributed to the proliferation and invasion of malignant glioma [38]. Shear force-activated Piezo1 regulates the biological function of endothelial cells and mediates physiological and pathological processes in the vascular tissue [39]. Accordingly, we hypothesized that there might be a certain interplay between Piezo1 and integrin-based mechanosensitive pathway, and their effects may participate in matrix stiffness-induced angiogenesis.

In this study, we developed a new orthotopic liver cancer SD rat model with high liver stiffness background and an in vitro fibronectin (FN)-coated cell culture system with different stiffness to explore the interplay between Piezo1 and integrin β1 in the mechanosensory pathway and their effects on HCC angiogenesis for better understanding of matrix stiffness-induced angiogenesis.

2 | MATERIALS AND METHODS

2.1 | The cancer genome atlas (TCGA) database

Clinical data of 372 HCC patients and their tumor gene expression profiles were downloaded from TCGA database. Since the expression levels of lysyl oxidase (LOX) and collagen 1 (COL1) can indicate the grade of matrix stiffness [40, 41], the median expression values of LOX and collagen 1A1 (COL1A1) were taken as the threshold to stratify the patients. Of the 372 patients, 119 with $COL1A1^{High}$-LOX^{High} HCC were classified as the high stiffness group, 120 with $COL1A1^{Low}$-LOX^{Low} HCC were classified as the low stiffness group, and the rest 133 were excluded due to an inconsistent expression trend between COL1A1 and LOX. The mRNA expression levels of target genes, Piezo1, CD31, CD34 and vascular endothelial growth factor A (VEGFA), were compared between the two groups.

2.2 | Cells and cell culture

Two human HCC cell lines, MHCC97H cells and Hep3B cells, were obtained from the Liver Cancer Institute of Fudan University (Shanghai, China) and Cell Bank of Shanghai Institute of Biochemistry and Cell Biology (Shanghai, China), respectively. MHCC97H cells were cultured in Dulbecco's Modified Eagle's Medium (DMEM, Gibco, New York, NY, USA) supplemented with 10% fetal bovine serum (FBS, Biowest, Riverside, MO, USA) and 1% penicillin/streptomycin (Gibco), and Hep3B cells in Minimum Essential Medium (Gibco) with 12.5% FBS and 1% penicillin/streptomycin. HUVECs, purchased from ScienCell Research Laboratories, Inc, were cultured in endothelial cell medium (ScienCell, San Diego, CA, USA) with 5% FBS (ScienCell), 1% penicillin/streptomycin (ScienCell), and 1% endothelial cell growth supplement (ScienCell). Buffalo rat HCC cells McA-RH7777, acquired from the American Type Culture Collection (Manassas, VA, USA), were grown in the same culture medium as MHCC97H cells.

2.3 | Establishment of SD rat HCC models with high or normal liver stiffness background

For SD rat HCC models with high liver stiffness background, 5-week-old male SD rats (Shanghai JieSiJie Laboratory Animal Co., Ltd., Shanghai, China) were subcutaneously injected with 100% carbon tetrachloride (CCl_4) (3 mL/kg) in the abdomen, and then injected with 50% CCl_4 olive solution (2 mL/kg) twice a week. Twelve weeks later, SD rat models with high liver stiffness were formed, their liver stiffness was evaluated by liver elasticity ultrasound, and the expression of COL1 and LOX in HCC tissues was evaluated by immunohistochemical staining.

From two days before transplantation to three days after transplantation, the rats were intramuscularly injected with 2.5 mg dexamethasone per day. Approximately 1.6×10^6 McA-RH7777 cells mixed in Matrigel (BD Biosciences, Franklin, NJ, USA) were orthotopically injected under the capsule of rat liver. Penicillin (50,000 U/day) was used from the day of surgery to the second postoperative day to prevent infection. Twelve days later, orthotopic liver cancer SD rat models with high liver stiffness background were established, and their blood samples, tumors, and lung tissues were collected for further analysis.

The experimental method for the establishment of SD rat HCC models with normal liver stiffness background was the same as the method for orthotopic liver cancer SD rat models with high liver stiffness background, except for CCl_4-free pretreatment before transplantation.

All animal care and experiments used in the study followed the guideline for the Care and Use of Laboratory Animals published by the US National Academy of Science (Washington, WA, USA), and the experiment design of the animal model was approved by the Animal Care Ethical Committee of Zhongshan Hospital, Fudan University (Shanghai, China).

2.4 | Lentivirus infection

The target fragment of genes (Supplementary Table S1) and packaging recombinant plasmid of lentivirus were designed and constructed by GeneChem Co. Ltd. (Shanghai, China). The fragment targeting human gene integrin β1 was inserted into the plasmid pGCSIL, and the fragment targeting human gene Piezo1 was inserted into the GV112 vector. The target sequence to miR-625-5p was cloned into the GV280 vector, miR-625-5p overexpression sequence was inserted into GV369. The fragments targeting rat genes integrin β1 and Piezo1 were inserted into the GV112 vector, respectively. When HCC cells grew and reached 40% confluence, they were infected with lentivirus and selected by puromycin (2 μg/mL). The efficiency of inhibition or overexpression was evaluated by quantitative real-time polymerase chain reaction (qRT-PCR) and Western blotting.

2.5 | Hematoxylin-eosin (H&E) staining and Sirius red staining

H&E staining: Tissue sections were dewaxed with xylene and rehydrated with ethanol at different concentrations, and then they were stained with hematoxylin for 5 min and rinsed with running water. After that, they were stained with eosin for 2 min.

Sirius red staining: Slides were stained with Sirius red reagent (Polysciences Inc, Warrington, PA, USA) for 1 h, and then washed in acetic acid, dehydrated in ethanol, and cleared in xylene. Quantifications of collagen proportional area (CPA) were measured by ImageJ software (National Institutes of Health, Bethesda, MD, USA).

2.6 | Immunohistochemistry (IHC)

Immunohistochemical staining was the same as the method described previously [31]. The primary antibodies were diluted as follows: LOX (1:100, Abcam, Cambs, Cambridge, UK), COL1 (1:100, Affinity, Cincinnati, OH, USA), Piezo1 (1:50, Abcam), CD31 (1:100, Abcam), hypoxia inducible factor-1α (HIF-1α) (1:100, Abcam), VEGFA (1:100, Proteintech, Wuhan, Hubei, China), insulin-like growth factor binding protein 2 (IGFBP2) (1:200, BOSTER, Wuhan, Hubei, China), CXC chemokine ligand 16 (CXCL16) (1:200, Proteintech). Photos of representative sites were captured with an Olympus microscope (Tokyo, Japan). The density of positive staining was measured by ImageJ software. Microvascular density (MVD) was assessed based on IHC staining of CD31. The slides were examined under 100× magnification to identify the highest vascular density area (hot spot) within the tumor, and five areas of highest MVD under 200× magnification were selected to calculate the average MVD. The average MVD of the five areas was recorded as the MVD level.

2.7 | FN-coated substrate gels with different stiffness

FN-coated substrate gels with the stiffness of 6, 10, and 16 kPa were prepared as described previously [30]. The suspended HCC cells (1×10^6) in 0.6 mL culture medium were spread onto an FN-coated gel in a dish and cultured for

2-3 h at 37°C with 5% CO_2. Subsequently, 10 mL culture medium was added to the dish, and the attached cells were further cultured for 36-48 h at 37°C with 5% CO_2. Cells were collected from the gel surface with a cell scraper for the following analysis.

2.8 | Western blotting

Western blot was performed as in our previous work [18] with a little modification. Briefly, 100 μg protein extracted from HCC cells was loaded and resolved on sodium dodecyl sulfate polyacrylamide gel electrophoresis (SDS-PAGE) for Piezo1 detection, and 20 μg protein extract for other target protein detection. The conditions of membrane transfer were optimized as 350 mA, 210 min for Piezo1, 300 mA, 45 min for von Hippel-Lindau (VHL), 300 mA, and 90 min for other target proteins. The diluted primary antibodies were as follows: integrin β1 (1:1000, Cell Signal Technology, Boston, MA, USA), Piezo1 (1:500, Abcam), COL1 (1:1000, Affinity), α-tubulin (1:5000, Proteintech), HIF-1α (1:1000, Abcam), VHL (1:1000, Abcam), IGFBP2 (1:1000, Abcam), CXCL16 (1:1000, Abcam), L-vascular endothelial growth factor A (L-VEGFA) (1:1000, Proteintech), ubiquitin (UB) (1:1000, Cell Signal Technology). The secondary horseradish peroxidase (HRP)-conjugated antibody (Proteintech) was diluted at 1:5000.

2.9 | An HCC tissue microarray from buffalo rat HCC models with different liver stiffness backgrounds

An HCC tissue microarray was constructed previously [18] from buffalo rat HCC models with different liver stiffness backgrounds.

2.10 | HCC patients

Clinical data of 88 HCC patients who underwent curative resection at the Department of Liver Surgery, Zhongshan Hospital of Fudan University between January 2008 and December 2008 were analyzed. Patients were followed up till December 2013. HCC patients were diagnosed according to the diagnostic criteria of the American Association for the Study of Liver Diseases (2018) [42], and their clinical stage was determined according to the Barcelona Clinic Liver Cancer staging system (2004) [43] and the 8th edition of Tumor Node Metastasis (TNM) staging system [44], respectively. Tumor differentiation grade was evaluated by the Edmondson grading system [45]. Vascular invasion, tumor number, tumor size, and other clinical parameters such as age, gender, hepatitis B surface antigen (HBsAg), alpha-fetoprotein (AFP), and liver function indicators were collected for univariate and multivariate analyses.

2.11 | The miRTarBase database

Target microRNA (miRNA) to Piezo1 and COL1A1 genes were identified seperately from the miRTarBase database (https://miRTarBase.cuhk.edu.cn/). The common miRNAs targeting both Piezo1 and COL1A1 genes were identified.

2.12 | miRNA qRT-PCR

Total RNA was extracted from HCC cells using TRIzol reagent (Invitrogen). The cDNA of miRNA was reversely transcribed using All-in One^{TM} miRNA qRT-PCR Detection Kit 2.0 (GeneCopoeia, Rockville, MD, USA) according to the manufacturer's protocol. Specific primers for U6 and miR-625-5p were all synthesized by GeneCopoeia. Reaction conditions were performed following the manufacturer's protocol of GeneCopoeia. The target gene was amplified by a QuantStudio® 5 Real-Time PCR instrument (Thermo Fisher Scientific, Waltham, MA, USA) according to the manufacturer's protocol. Heterogeneous nuclear RNA (hsnRNA) U6 was selected as an endogenous reference. Relative gene expression was normalized to U6 and reported by $2^{-\Delta\Delta Ct}$ method.

2.13 | Recombinant plasmid construction and transient transfection

miR-625-5p interference sequence (5'-GGACUAUAGAACUUUCCCCCU-3') and its scramble sequence (5'- CAGUACUUUUGUGUAGUACAA-3') were constructed and synthesized by Sangon Biotech (Shanghai, China). When they grew and reached 80% confluence, the cells were transfected with a negative control siRNA or si-miR-625-5p in Opti-Medium at the concentration of 50 nmol/L via lipofectamine 2000 (Invitrogen).

2.14 | Dual-luciferase reporter assay

The wild-type Piezo1 3'-untranslated region (UTR) or COL1A1 3'-UTR containing the binding site of miR-625-5p and its mutant type were all designed and synthesized by OBiO Technology Co. Ltd. (Shanghai, China). 293T

cells were seeded into a 24-well culture plate on the day before plasmid transfection. The cells were transfected with the designed plasmids. After 48 h culture, the cells were harvested, and their luciferase activity was analyzed using the Dual-luciferase Reporter Assay System (Promega, Madison, WI, USA).

2.15 | Scanning electron microscopy (SEM)

Rat rail COL1 (3.58 mg/mL, Corning, New York, NY, USA) and serum-free DMEM were mixed in volume ratios of 1:20 and 1:4 to prepare two types of substrate gels for SEM analysis. The mixtures containing different amounts of COL1 on a slide were solidified into the gels at 4°C overnight. Then the gels were sampled and fixed in 2% glutaraldehyde at 4°C. Samples were stained with 1% osmium tetroxide and observed under a scanning electron microscope (JEOL, Tokyo, Japan).

2.16 | Collection of conditioned medium (CM) from shPiezo1-transfected MHCC97H cells

Wild-type, shCtrl-transfected, and shPiezo1-transfected MHCC97H cells were cultured on the high-stiffness substrate for 48 h, and their culture supernatants were collected and concentrated by a centrifugal filter (Millipore, Schwalbach, SL, Germany) at 4000 × g for 30 min at 4°C, and then the concentrated supernatant was filtered through 0.22 μm filters and stored at -80°C for subsequent use. The protein concentration of the concentrated supernatant was measured by bicinchoninic acid assay (Beyotime, Shanghai, China).

2.17 | Tube formation assay

HUVECs (5×10^5) suspended in extracellular matrix (ECM) containing CM were seeded onto a Matrigel-coated dish. After 8 h culture, tube-like structures on Matrigel were photographed by an inverted microscope (Olympus). The state of tube forming in the picture was analyzed using ImageJ software.

2.18 | Wound healing assay

Wound healing assay was performed to assess the effect of CM intervention on cell migration. After HUVECs grew to reach a tight cell monolayer in a 6-well plate, the cell monolayer was scratched with a plastic pipette tip. The remaining cells were washed twice with PBS and then treated with CM for 48 h. The migrated cells at the wound front were photographed using an Olympus microscope and analyzed by ImageJ software.

2.19 | Analysis of angiogenesis-related factors in CM using a human angiogenesis array

Angiogenesis-related factors in CM were analyzed by Human Angiogenesis Array Kit (Proteome Profiler^{TM}, R&D Systems, Minneapolis, MN, USA). Samples were mixed with a detection antibody cocktail for 1 h. The sample/antibody mixture was then incubated with an angiogenesis array overnight at 4°C. After unbound materials were removed from the array, streptavidin-HRP and chemiluminescent detection reagents were sequentially added. Array signals were recorded by the Bio-Rad Chemi Doc XRS imaging system (Hercules, CA, USA) and analyzed using ImageJ software.

2.20 | Intracellular Ca^{2+} measurement

HCC cells were cultured on different stiffness substrates for 24 h, and then their culture solution was replaced with a fresh culture medium containing Ca^{2+} probe (Ca^{2+}-GPCR analysis-calcium ion indicator probe Fluo-4, AM, KeyGEN BioTECH, Nanjing, China, 1 μmol/L). The cells were further cultured for 30 min, and the culture medium was discarded. The cells were washed once with PBS and cultured in a fresh culture medium for 1 h. The fluorescence intensity of intracellular Ca^{2+} in HCC cells was observed and recorded by a fluorescence microscope (Olympus) with cellSens software (Olympus).

2.21 | Intervention of Yoda1, GsMTx4 and MG132

Yoda1 (an agonist for Piezo1, MedChemExpress, Shanghai, China, 25 μmol/L for MHCC97H and 5 μmol/L for Hep3B) and GsMTx4 (an antagonist for Piezo1, Abcam, 2.5 μmol/L for both MHCC97H and Hep3B) were respectively applied to treat HCC cells grown on different stiffness substrates for exploring the effect of Piezo1 activation on pro-angiogenic factor expression. MG132 (a proteasome inhibitor, Cell Signal Technology, 10 μmol/L) was applied to treat HCC cells grown on different stiffness substrates for exploring the effects of Piezo1 and matrix stiffness on HIF-1α ubiquitination.

2.22 | Co-immunoprecipitation (Co-IP)

Total protein was extracted from the cells using immunoprecipitation lysis buffer (20 mmol/L Tris-HCl, pH 7.6; 150 mmol/L NaCl; 1 mmol/L ethylene diamine tetraacetic acid (EDTA); 0.5% NP-40; 10% glycerol; 1 mmol/L phenylmethanesulfonyl fluoride). The extracted protein was pretreated with protein A/G plus-agarose beads (Millipore) overnight at 4°C. Subsequently, these mixtures were incubated with IgG or HIF-1α antibody at 4°C for 24 h, respectively. Afterwards, the collected beads were washed three times using washing buffer (50 mmol/L Tris-HCl, pH 7.6; 300 mmol/L NaCl; 1 mmol/L EDTA; 0.5% NP-40; 10% glycerol), and the post-elution beads were boiled in the loading buffer, resolved on SDS-PAGE. Immunoblotting was finally performed to detect VHL and HIF-1α.

2.23 | Statistical analysis

GraphPad Prism 8.0 (San Diego, CA, USA) and SPSS 22.0 statistical software (SPSS, Chicago, IL, USA) were used for all statistical analyses. Data are presented as mean ± standard deviation (SD). Quantitative variables were analyzed by the analysis of variance (ANOVA) test among three groups and Student's *t*-test between two groups. Qualitative variables were analyzed by the chi-squared test and rank sum test. Kaplan-Meier analysis and log-rank test were performed to evaluate the association between Piezo1 expression and patients' overall survival (OS). The interval time of OS was calculated from surgery to death of any reason or the most recent follow-up. COX regression model was performed to clarify the prognostic value of Piezo1 expression. $P < 0.05$ was considered statistically significant.

3 | RESULTS

3.1 | Piezo1 participated in matrix stiffness-induced angiogenesis and metastasis

On the basis of our previous findings that increased matrix stiffness potentiated HCC angiogenesis [31, 32], we further explored the contribution of Piezo1 to matrix stiffness-induced angiogenesis in HCC. We first downloaded clinical data of 372 HCC patients and their tumor gene expression profiles from the TCGA database to clarify Piezo1 expression and its association with HCC angiogenesis. Considering that the expression levels of LOX and COL1 can indicate the grade of matrix stiffness [40, 41], we used the median expression values of LOX and COL1A1 as the threshold to stratify HCC patients into $COL1A1^{High}$-LOX^{High} group (119 patients) and $COL1A1^{Low}$-LOX^{Low} group (120 patients). Compared with that in the $COL1A1^{Low}$-LOX^{Low} TCGA-HCC tissues, Piezo1 presented an obvious upregulation in $COL1A1^{High}$-LOX^{High} TCGA-HCC tissues (Figure 1A), and its high expression was associated with an unfavorable prognosis (Figure 1B). Additionally, CD31, CD34, and VEGFA also exhibited higher expression in $COL1A1^{High}$-LOX^{High} TCGA-HCC tissues than in $COL1A1^{Low}$-LOX^{Low} TCGA-HCC tissues (Figure 1A), in agreement with our previous results in rat HCC tissues [31, 32]. Importantly, Piezo1 was positively associated with CD31 in expression level (Figure 1C). These results described above suggest a potential linkage between Piezo1 and matrix stiffness-induced HCC angiogenesis.

Subsequently, we developed new orthotopic liver cancer SD rat models with high and normal liver stiffness backgrounds (Figure 1D and Supplementary Figure S1A) to validate the role of Piezo1 in matrix stiffness-induced angiogenesis and metastasis. We first compared liver stiffness levels of SD rat models with high or normal liver stiffness background (healthy liver) using LOX/COL1 expression (Supplementary Figure S1B) and sirius red staining (Supplementary Figure S1C). SD rats with high liver stiffness background had higher expression of LOX and COL1 and more collagen fibers in tumor tissues than those with normal liver stiffness background (Supplementary Figure S1B-C). Then we detected the stiffness of SD rats with high liver stiffness background using liver elasticity ultrasound and found that the mean stiffness value of SD rats with high liver stiffness background (17.04 ± 1.73 kPa) could represent the tissue stiffness of advanced cirrhosis [46]. These results suggested that liver stiffness levels of the established SD rat models with high liver stiffness background were able to mirror the stiffness ranges of advanced cirrhosis, which were in accordance with reported data [40, 41, 46]. Afterwards, by hepatic subcapsular injection of HCC cells combined with short-term usage of dexamethasone, we successfully obtained orthotopic liver cancer SD rat models with high liver stiffness background (Figure 1D, Supplementary Figure S1A) and ascertained that their serum phenotype (Supplementary Figure S1D) was almost consistent with that of HCC patients with advanced cirrhosis [47]. So, the established animal models can simulate the pathological properties of HCC with advanced cirrhosis. Using shPiezo1-transfected McA-RH7777 cells or shITGB1-transfected McA-RH7777 cells (Figure 1E), we also assessed the roles of Piezo1 or integrin β1 in matrix stiffness-regulated HCC angiogenesis and discovered that tumor volume of the shPiezo1 #1 group was significantly smaller than those of the two control groups (Figure 1F). Simultaneously, the positive

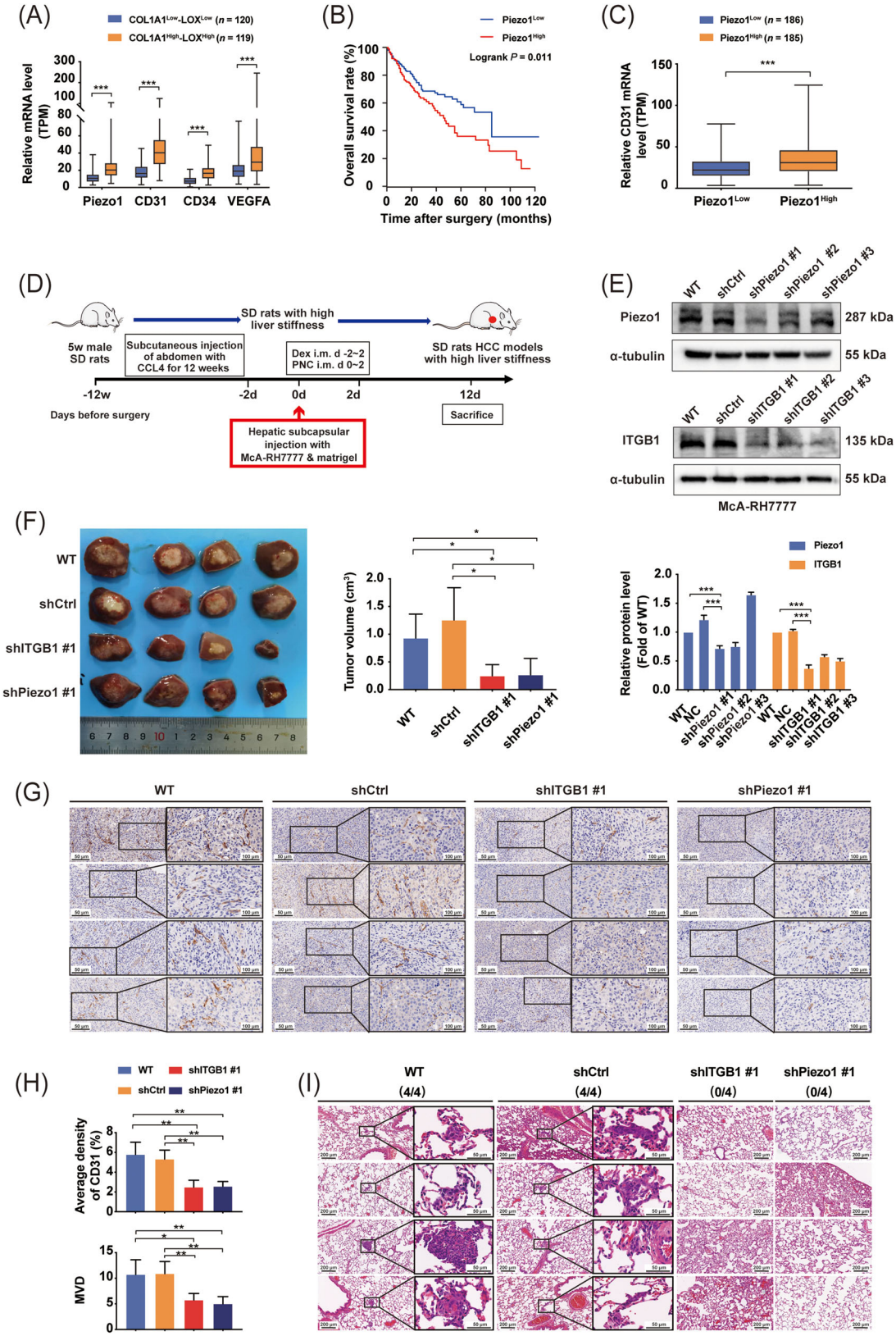

FIGURE 1 Piezo1 participates in matrix stiffness-induced angiogenesis and facilitates metastasis. (A) The expression levels of Piezo1, CD31, CD34 and VEGFA were markedly increased in COL1A1^{High}-LOX^{High} TCGA-HCC tissues ($n = 119$) compared with those in COL1A1^{Low}-LOX^{Low} TCGA-HCC tissues ($n = 120$). (B) High expression of Piezo1 was significantly associated with short overall survival in TCGA-HCC patients. (C) CD31 was significantly overexpressed in the Piezo1^{High} group ($n = 185$) compared with the Piezo1^{Low} group ($n = 186$) in the TCGA-HCC cohort. (D) A flow diagram for the establishment of orthotopic liver cancer SD rat models with high liver stiffness

expression area of CD31 and the microvascular density (MVD) in HCC tissues of the shPiezo1 #1 group dropped considerably (Figure 1G-H), and Piezo1 suppression evidently hindered the incidence of lung metastasis (Figure 1I), revealing that Piezo1 mediates matrix stiffness-induced HCC angiogenesis and influences the incidence of lung metastasis. On the other hand, knockdown of integrin β1, a stiffness-sensor molecule identified previously [18, 31], also resulted in an apparent decline in tumor growth, angiogenesis, and lung metastasis (Figure 1F-I), which verified that increased matrix stiffness promoted angiogenesis and metastasis via integrin β1. In orthotopic liver cancer SD rat models with normal liver stiffness background (Supplementary Figure S1A), knockdown of Piezo1 or integrin β1 also significantly inhibited tumor growth and angiogenesis (Supplementary Figure S2A-F), but they had little effect on the occurrence of lung metastasis (Supplementary Figure S2G), which were significantly different from the results of the SD rat model with high liver stiffness background. These results indirectly support that higher liver stiffness facilitated the occurrence of lung metastasis in HCC, which were consistent with our previous findings in buffalo rat HCC models [18]. Taken together, in addition to integrin β1, Piezo1 may also play a regulatory role in matrix stiffness-driven angiogenesis and metastasis in HCC.

3.2 | Piezo1 expression in HCC cells under different stiffness stimulation and its clinical significance

We applied 6, 10, and 16 kPa stiffness substrates, which represented the stiffness levels of normal, fibrotic, and cirrhotic liver tissues [46, 48, 49], to analyze matrix stiffness-mediated effects on Piezo1 expression in HCC cells. The expression levels of Piezo1 and COL1 in HCC cells all showed an increasing trend with the increase of matrix stiffness (Figure 2A). Integrin β1 suppression remarkably reduced the expression of Piezo1 and COL1 in HCC cells grown on a high-stiffness substrate (Figure 2B). Similarly, in a rat HCC tissue microarray analysis, Piezo1 also presented a significant upregulation in HCC tissues with high liver stiffness background compared with that in HCC tissues with normal and medium liver stiffness background (Figure 2C). Because high expression of COL1 and LOX in rat HCC tissues with high liver stiffness background has been validated in our previous study [18], we easily inferred that Piezo1 expression level was associated with matrix stiffness level or COL1/LOX expression level. Additionally, high Piezo1 expression in $COL1^{High}$-LOX^{High} human HCC tissues (44 cases) (Figure 2D-E) also supported an association between Piezo1 expression and COL1 expression. Thereby, at cellular and tissue levels, increased matrix stiffness indeed promoted Piezo1 and COL1 expression, and both of them showed the same trend in the expression levels.

To evaluate the clinical significance of Piezo1 in HCC patients, we used the median expression value of Piezo1 in HCC tissues as the cut-off value to divide HCC patients into the $Piezo1^{High}$ group (44 cases) and the $Piezo1^{Low}$ group (44 cases). The results demonstrated that high expression of Piezo1 was associated with high LOX/COL1 expression, cirrhosis-associated indexes (total bilirubin, albumin), AFP, and tumor size (Table 1), in accordance with the above-mentioned results in orthotopic liver cancer SD rat models. Additionally, $Piezo1^{High}$ HCC patients had an unfavorable prognosis (Figure 2F), which was identical to the result of the TCGA analysis. Multivariate analysis suggested that apart from TNM stage and vascular invasion, Piezo1 overexpression also served as an independent risk factor for OS of HCC patients (Supplementary Table S2).

3.3 | A positive feedback loop worked in matrix stiffness-mediated Piezo1 upregulation

Given that Piezo1 and COL1 were all highly expressed in HCC cells under high-stiffness stimulation (Figure 2A), and the alteration of liver matrix stiffness was mainly attributed to extracellular matrix protein COL1 deposition

background. (E) shPiezo1-transfected (top panel) and shITGB1-transfected (bottom panel) McA-RH7777 cell lines were verified by Western blotting. The protein quantification of Piezo1 and ITGB1 in shPiezo1-transfected and shITGB1-transfected McA-RH7777 cells was analyzed by ImageJ software. (F) Gross appearance of orthotopic HCC tumors and the tumor volumes in WT, shCtrl, shITGB1 #1 and shPiezo1 #1 groups with high liver stiffness background (4 rats/group). (G) Representative images of CD31-positive area in orthotopic HCC tumors in WT, shCtrl, shITGB1 #1 and shPiezo1 #1 groups with high liver stiffness background. (H) Quantitative analysis of CD31-positive area and MVD in orthotopic HCC tumors of WT, shCtrl, shITGB1 #1 and shPiezo1 #1 groups with high liver stiffness background. (I) Lung metastasis of orthotopic HCC tumors in WT, shCtrl, shITGB1 #1 and shPiezo1 #1 groups with high liver stiffness background. No rats in the shITGB1 #1 and shPiezo1 #1 groups and all rats in the WT and shCtrl groups had developed lung metastasis. *$P < 0.05$, ** $P < 0.01$, ***$P < 0.001$.
Abbreviations: VEGFA, vascular endothelial growth factor A; TCGA, the Cancer Genome Atlas; HCC, hepatocellular carcinoma; COL, collagen; LOX, lysyl oxidase; WT, wild type; Ctrl, control; ITGB1, integrin β1; MVD, microvascular density.

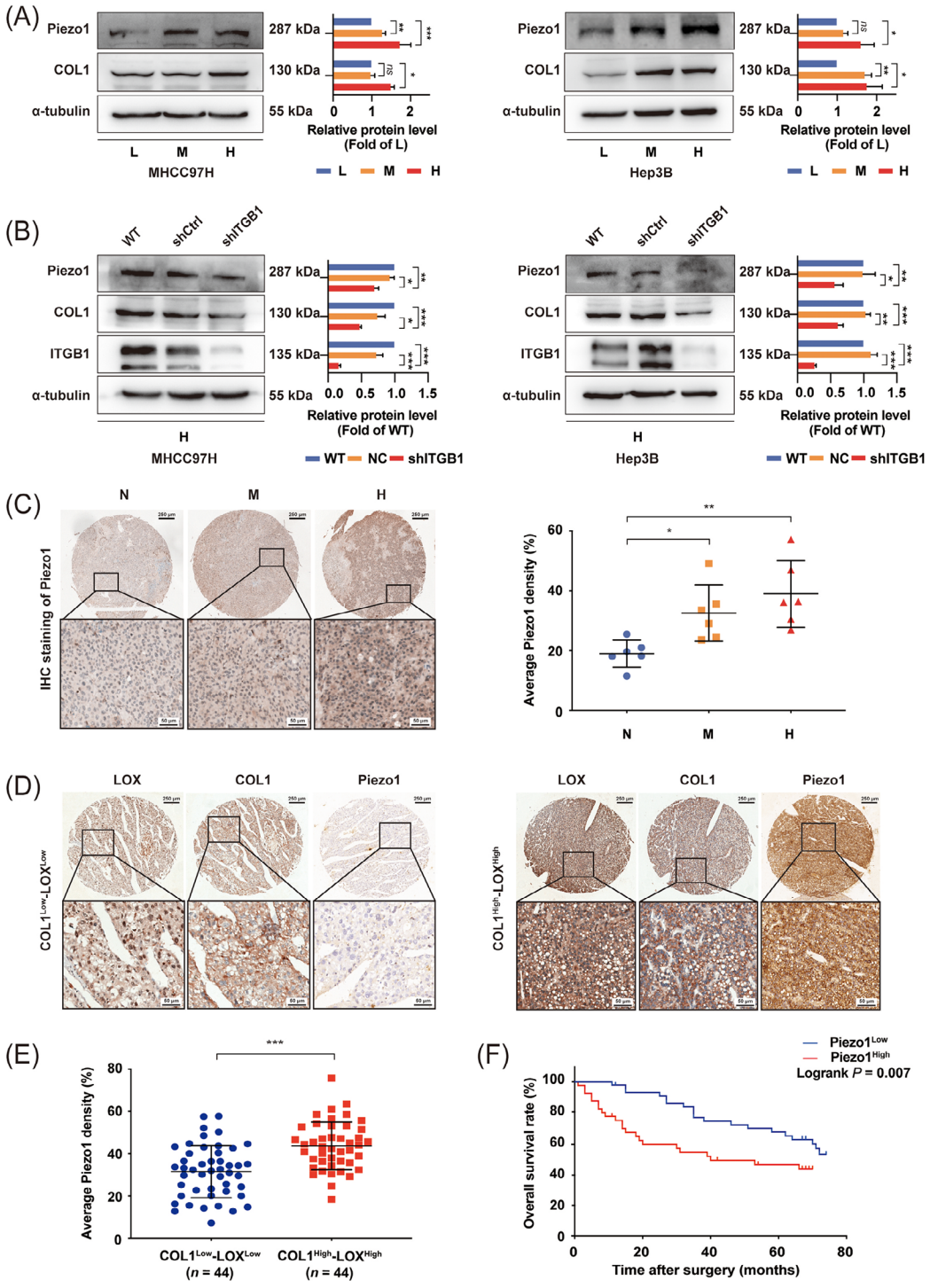

FIGURE 2 Piezo1 expression levels in HCC in vivo and in vitro and its clinical significance. (A) The expression of Piezo1 and COL1 in MHCC97H cells and Hep3B cells grown on different stiffness substrates. (B) Knockdown of integrin β1 partially decreased the expression of Piezo1 and COL1 in MHCC97H cells and Hep3B cells grown on high-stiffness substrate. (C) Piezo1 expression in an HCC tissue microarray derived from buffalo rat HCC models with different liver stiffness backgrounds. (D-E) Representative images of immunohistochemistry staining of Piezo1 in COL1^{High}-LOX ^{High} human HCC tissues ($n = 44$) and COL1^{Low}-LOX ^{Low} human HCC tissues ($n = 44$). (F) High expression of Piezo1 was significantly associated with poor overall survival in HCC patients. The protein expression and Piezo1-staining density were quantified using ImageJ software. *ns*, not significant, * $P < 0.05$, ** $P < 0.01$, *** $P < 0.001$.

Abbreviations: L, low stiffness (6 kPa); M, medium stiffness (10 kPa); H, high stiffness (16 kPa); ITGB1, integrin β1; HCC, hepatocellular carcinoma; N, normal stiffness; WT, wild type; Ctrl, control; COL1, collagen 1; LOX, lysyl oxidase.

TABLE 1 Associations of Piezo1 expression with clinicopathologic characteristics in HCC tissues

Variable	Piezo1 expression		*P* value
	Low	High	
Total (cases)	44	44	
Age [years; median (range)]	53 (27-79)	50 (19-78)	0.111
Gender [cases (%)]			0.280
Male	38 (86.4)	33 (75.0)	
female	6 (13.6)	11 (25.0)	
TB [cases (%)]			0.011
≤17.1 μmol/L	41 (93.2)	31 (70.5)	
>17.1 μmol/L	3 (6.8)	13 (29.5)	
Albumin (g/L; mean ± SD)	10.0 ± 14.0	18.3 ± 17.3	<0.001
ALT (U/L; mean ± SD)	42.1 ± 28.4	45.7 ± 36.0	0.644
PT (s; mean ± SD)	12.9 ± 0.9	12.9 ± 0.9	0.834
HBV infection [cases (%)]			0.196
Negative	8 (18.2)	3 (6.8)	
Positive	36 (81.8)	41 (93.2)	
AFP (ng/mL; mean ± SD)	5320.9 ± 13217.0	10887.6 ± 18174.4	0.005
Tumor size (cm; mean ± SD)	6.4 ± 2.8	7.3 ± 4.8	0.007
Tumor number (mean ± SD)	1.3 ± 0.7	1.7 ± 1.9	0.075
Histological grade			
[cases (%)]			0.171
I	0 (0.0)	1 (2.3)	
II	37 (84.1)	30 (68.2)	
III	7 (15.9)	13 (29.5)	
TNM stage [cases (%)]			0.132
I	21 (47.7)	20 (45.5)	
II	16 (36.4)	10 (22.7)	
III	6 (13.6)	14 (31.8)	
IV	1 (2.3)	0 (0.0)	
BCLC stage [cases (%)]			0.730
A	18 (40.9)	15 (34.1)	
B	21 (47.7)	22 (50.0)	
C	5 (11.4)	7 (15.9)	
Thrombi [cases (%)]			0.438
No	26 (59.1)	29 (65.9)	
Microscopic	14 (31.8)	9 (20.5)	
Branch	4 (9.1)	6 (13.6)	
LOX/COL1 expression			
[cases (%)]			0.001
Low	31 (70.5)	13 (29.5)	
High	13 (29.5)	31 (70.5)	

HCC, hepatocellular carcinoma; No, number; TB, total bilirubin; ALT, alanine aminotransferase; PT, prothrombin time; HBV, hepatitis B virus; AFP, alpha-fetoprotein; TNM, Tumor Node Metastasis; BCLC, Barcelona Clinic Liver Cancer; LOX, lysyl oxidase; COL1, collagen 1.

and crosslinking [40, 41], we speculated that there might be a positive feedback regulation loop in matrix stiffness-mediated effect on Piezo1 upregulation. Specifically, matrix stiffness promoted Piezo1 expression, simultaneously enhanced the production of extracellular COL1, and COL1-reinforced tissue stiffening resulted in more expression of Piezo1. Considering that the same miRNA can concurrently regulate different target proteins, we identified 6 common miRNAs from the miRTarBase database that could target both Piezo1 and COL1A1 genes (Figure 3A). Among them, we determined miR-625-5p as the target miRNA by literature review and preliminary experiment analysis and then elucidated its role in matrix stiffness-upregulated Piezo1. Increased matrix stiffness restrained miR-625-5p expression in HCC cells (Figure 3B and Supplementary Figure S3A), and suppression of integrin β1 significantly reversed high-stiffness stimulation-induced miR-625-5p downregulation (Figure 3C and Supplementary Figure S3B). The expression trend of miR-625-5p was opposite to that of Piezo1 and COL1 mentioned above (Figure 2A). These data indicate that there may exist a negative regulation of miR-625-5p on Piezo1 and COL1 expression under different stiffness stimulation.

Based on the predicted binding sites of miR-625-5p to the 3'-UTR of Piezo1 and COL1A1 (Figure 3D-E), we respectively constructed the wild-type recombinant plasmids (WT Piezo1 3'-UTR and WT COL1A1 3'-UTR) and the mutant-type recombinant plasmids (MUT Piezo1 3'-UTR and MUT COL1A1 3'-UTR) to analyze whether there was a binding site between miR-625-5p and the 3'-UTR regions of these two target genes. Dual-luciferase reporter assay for Piezo1 and miR-625-5p showed that the luciferase fluorescence intensity of the miR-625-5p mimics group was decreased by 40.55% compared with that of the control group ($P < 0.001$), while the luciferase fluorescence intensity of the MUT Piezo1 3'-UTR group was partially restored compared with that of the WT Piezo1 3'-UTR group ($P < 0.001$) (Figure 3D). Similarly, for miR-625-5p and COL1A1 3'-UTR, the luciferase fluorescence intensity of the miR-625-5p mimics group was decreased by 38.66% ($P < 0.001$), and the luciferase fluorescence intensity of the MUT COL1A1 3'-UTR group was also partially restored ($P < 0.001$) (Figure 3E). The above results supported that miR-625-5p is specifically bound to the 3'-UTR sites of Piezo1 or COL1A1. However, a partial reversion but not full reversion in the MUT Piezo1 3'-UTR group or the MUT COL1A1 3'-UTR group implied that other atypical binding sites might exist except the predicted binding sites. We further analyzed the regulatory role of miR-625-5p in matrix stiffness-upregulated Piezo1 and found that miR-625-5p overexpression distinctly decreased the expression of Piezo1 and COL1 in HCC cells grown on high-stiffness substrate (Figure 3F-G and Supplementary Figure S3C-F). Conversely, miR-625-5p inhibition improved Piezo1 and COL1 expression in HCC cells grown on low-stiffness substrate (Figure 3H-I and Supplementary Figure S3G-J). All these results demonstrated that miR-625-5p participated in matrix stiffness-upregulated Piezo1 and COL1.

To assess the effect of COL1 deposition on matrix stiffness level, we prepared two types of substrate gel by mixing COL1 and serum-free DMEM in a volume ratio of 1:20 and 1:4 to simulate different deposition amounts of COL1. The results showed that the stiffness level of the substrate gel (1:4, 1230.190 Pa) was significantly higher than that of the substrate gel (1:20, 341.522 Pa), and collagen I fiber bundles of the substrate gel (1:4) were thicker and more tightly packed than that of the substrate gel (1:20) (Figure 3J-K). It confirmed our speculation that COL1 deposition reinforced tissue stiffening. Together, we proposed that a positive feedback regulation loop as stiff matrix/integrin β1/miR-625-5p/Piezo1 and COL1/stiffer matrix was involved in matrix stiffness-upregulated Piezo1 in HCC (Figure 3L).

3.4 | Differentially expressed angiogenesis-related cytokines between shPiezo1-CM and Scramble-CM

Paracrine is the most frequent regulatory way for tumor cells to induce angiogenesis [50–52]. The above results in animal models and HCC tissues suggested that Piezo1 might participate in matrix stiffness-induced angiogenesis. By comparing the inhibitory effects of three knockdown clones for Piezo1 in HCC cells, the one with the best inhibitory effect was selected for subsequent function analysis (shPiezo1 #2 for MHCC97H cells and shPiezo1 #3 for Hep3B cells, Figure 4A). Subsequently, the CM from wild-type, shCtrl-transfected, and shPiezo1 #2-transfected MHCC97H cells grown on high-stiffness substrate (WT-CM, Scramble-CM, and shPiezo1-CM) were collected to appraise their effects on angiogenesis. Compared with the cells treated with shPiezo1-CM, HUVECs treated with WT-CM and Scramble-CM all presented stronger abilities in tube formation (Figure 4B) and migration (Figure 4C), illustrating that WT-CM and Scramble-CM contained more pro-angiogenic factors than shPiezo1-CM. Thereby, Piezo1 upregulation may influence the expression and secretion of pro-angiogenic factors and promote HCC angiogenesis. Using a human angiogenesis array comprising 55 cytokines, we successfully found out 9 differentially expressed pro-angiogenic and anti-angiogenic factors (fold change >1.2 or <0.5) between shPiezo1-CM and Scramble-CM (Figure 4D and Supplementary Table S3), including 7 downregulated factors (Serpin F1, CXCL16, IGFBP-2, VEGF, PDGF-AA, IGFBP-3, interleukin-8) and 2

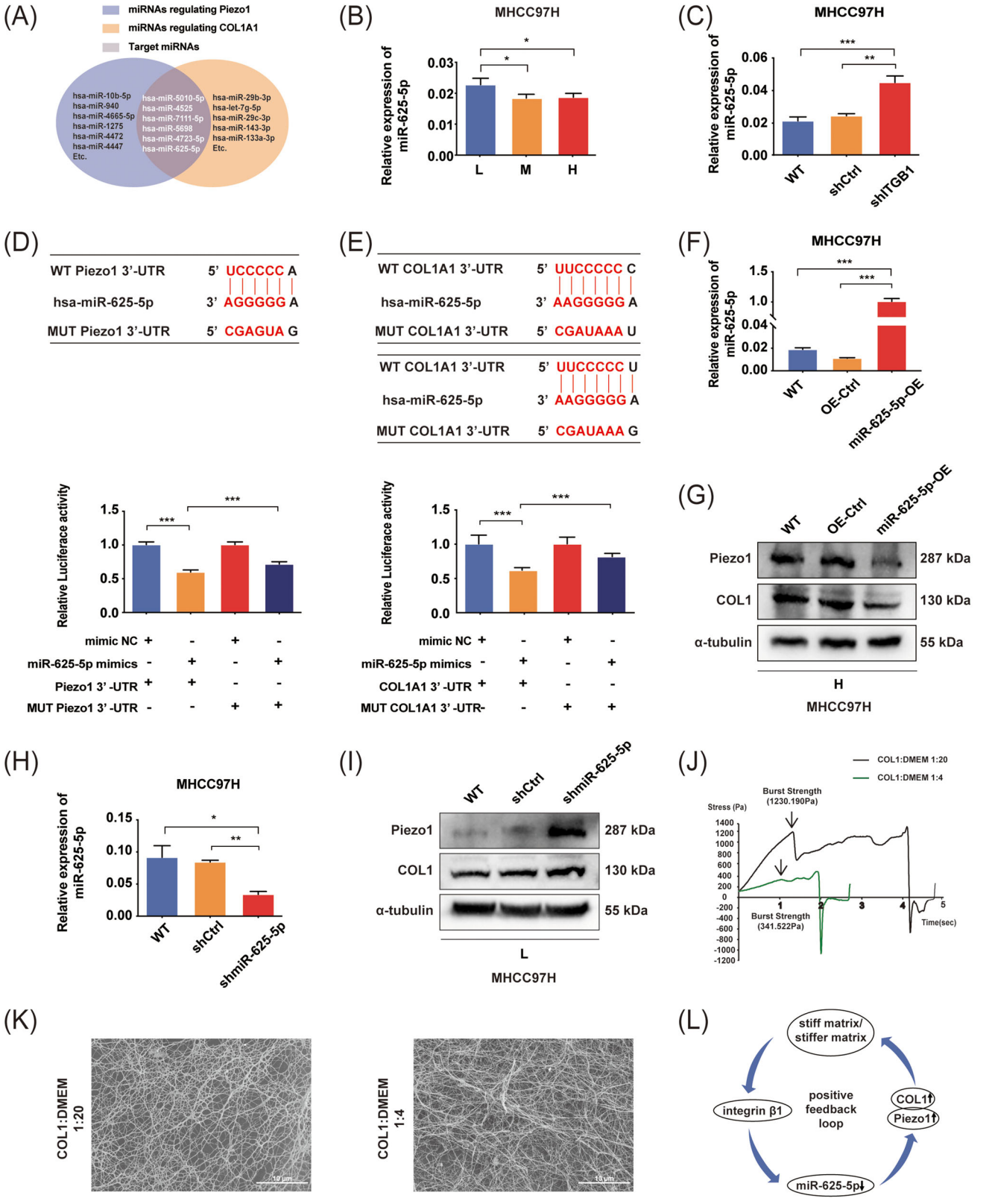

FIGURE 3 A positive feedback loop mediates matrix stiffness-induced Piezo1 upregulation. (A) The predicted miRNAs for two target genes Piezo1 and COL1A1 from the miRTarBase database. (B) The miRNA expression of miR-625-5p in MHCC97H cells cultured on different stiffness substrates detected by qRT-PCR. (C) Knockdown of integrin β1 significantly decreased miR-625-5p expression in MHCC97H cells cultured on high-stiffness substrate. (D-E) Luciferase assay showed that miR-625-5p specifically bound to the 3'-UTR of Piezo1 and COL1A1. (F) miR-625-5p-OE MHCC97H cells were verified by qRT-PCR. (G) Western blotting assay detected that Piezo1 and COL1 expression was decreased in miR-625-5p-OE MHCC97H cells grown on high-stiffness substrate. (H) miR-625-5p-knockdown MHCC97H cells were verified by

upregulated factors [Amphiregulin, urokinase-type plasminogen activator (UPA)] in shPiezo1-CM. Among these differentially expressed angiogenesis-related cytokines, most pro-angiogenic factors in shPiezo1-CM exhibited a decreasing trend in content. Based on the above results, we concluded that the overall effect of shPiezo1-CM was angiogenesis inhibition, and shPiezo1-CM lacked the pro-angiogenic factors required for tube formation and migration of HUVECs. Furthermore, we selected three differentially expressed pro-angiogenic factors, VEGF, CXCL16, and IGFBP2, as the target factors for subsequent validation. The reasons for this selection were as follows: (1) the evidence presented above suggested that Piezo1 was a pro-angiogenic regulator and mediated matrix stiffness-induced angiogenesis; (2) VEGF, IGFBP2, and CXCL16 had a common upstream transcription factor hypoxia-inducible factor (HIF-1α) [15, 16, 53, 54] and affected tumor proliferation, angiogenesis, invasion and metastasis [55–57]; (3) HIF-1α expression was not always dependent on hypoxia [58], and a variety of growth factors and cytokines were able to stabilize HIF-1α under normoxic conditions [58]; (4) increased matrix stiffness also played a regulatory role in HIF-1α expression in the polarized M2 macrophages [59]. In validation analysis, knockdown of Piezo1 remarkably suppressed the expression of VEGF, CXCL16, and IGFBP2 in HCC cells cultured on a high-stiffness substrate (Figure 4E), which was consistent with the results of the human angiogenesis array. Besides that, integrin β1 knockdown also partially attenuated the expression of VEGF, CXCL16, and IGFBP2 in HCC cells grown on a high-stiffness substrate (Figure 4F), meaning that matrix stiffness was also involved in the regulation of angiogenesis-related molecules. Consequently, knockdown of Piezo1 reduced the expression of angiogenesis-related cytokines and restrained matrix stiffness-induced HCC angiogenesis.

3.5 | Piezo1 activation and Ca^{2+} influx in HCC cells under high-stiffness stimulation

Under mechanical stimulation, Piezo1 allows the influx of positively charged ions (Ca^{2+}, Na^{+}) into the cells, and the content of Ca^{2+} influx can reflect the activation level of Piezo1 [34]. As shown in Figure 2A, increased matrix stiffness significantly upregulated Piezo1 expression. Accordingly, the relationship between Piezo1 expression and Piezo1 activation becomes an unavoidable problem for understanding the contribution of Piezo1 to matrix stiffness-induced HCC angiogenesis. We analyzed the levels of Ca^{2+} influx in HCC cells cultured on different stiffness substrates and discovered that the fluorescence intensity of Ca^{2+} in HCC cells was increased significantly with the increase of matrix stiffness (Figure 5A). Instead, suppressing Piezo1 significantly diminished the fluorescence intensity of Ca^{2+} in HCC cells cultured on the high-stiffness substrate (Figure 5B). It suggests that Ca^{2+} influx positively correlate with Piezo1 expression and matrix stiffness. On the other hand, Yoda1 intervention noticeably enhanced the fluorescence intensity of Ca^{2+} in HCC cells grown on low-stiffness substrate (Figure 5C), whereas GsMTx4 intervention clearly reduced it in HCC cells grown on high-stiffness substrate (Figure 5D). Overall, high-stiffness stimulation significantly enhanced Piezo1 expression and activation in HCC cells, and the expression level of Piezo1 was associated with its activation level under high-stiffness stimulation.

3.6 | Matrix stiffness-caused Piezo1 activation regulated HIF-1α ubiquitination and the expression of its downstream pro-angiogenic factors in HCC cells

HIF-1α, an important common transcription factor, governs the expression of many pro-angiogenic factors such as VEGF, CXCL16, and IGFBP2 [16, 55, 60]. We first elucidated whether matrix stiffness-caused Piezo1 activation regulated the expression of HIF-1α and its downstream pro-angiogenic factors. As shown on Figure 6A and Supplementary Figure S4A-B, high-stiffness stimulation significantly upregulated the expression of HIF-1α and its downstream target genes (VEGF, IGFBP2 and CXCL16) and significantly attenuated the expression of VHL (VH the E3 ligase of HIF-1α) in HCC cells, suggesting a potential linkage between high matrix stiffness and HIF-1α ubiquitination. Subsequently, we used proteasome inhibitor MG132 to treat HCC cells cultured on low-stiffness

qRT-PCR. (I) Western blotting assay detected that Piezo1 and COL1 expression was increased in miR-625-5p-knockdown MHCC97H cells grown on low-stiffness substrate. (J) Stiffness values of gels with different concentrations of collagen 1 (1:4 and 1:20) by a texture analyzer. (K) Representative images of gels made of COL1 and serum-free DMEM at volume ratios of 1:20 and 1:4 through SEM. (L) Schematic diagram of a positive feedback loop working in matrix stiffness-upregulated Piezo1 expression. * $P < 0.05$, ** $P < 0.01$, *** $P < 0.001$.

Abbreviations: L, low stiffness (6 kPa); M, medium stiffness (10 kPa); H, high stiffness (16 kPa); COL1, collagen1; WT, wild type; Ctrl, control; OE, overexpression; HCC, hepatocellular carcinoma; COL1, collagen 1; SEM, scanning electron microscopy; DMEM, dulbecco's modified eagle's medium.

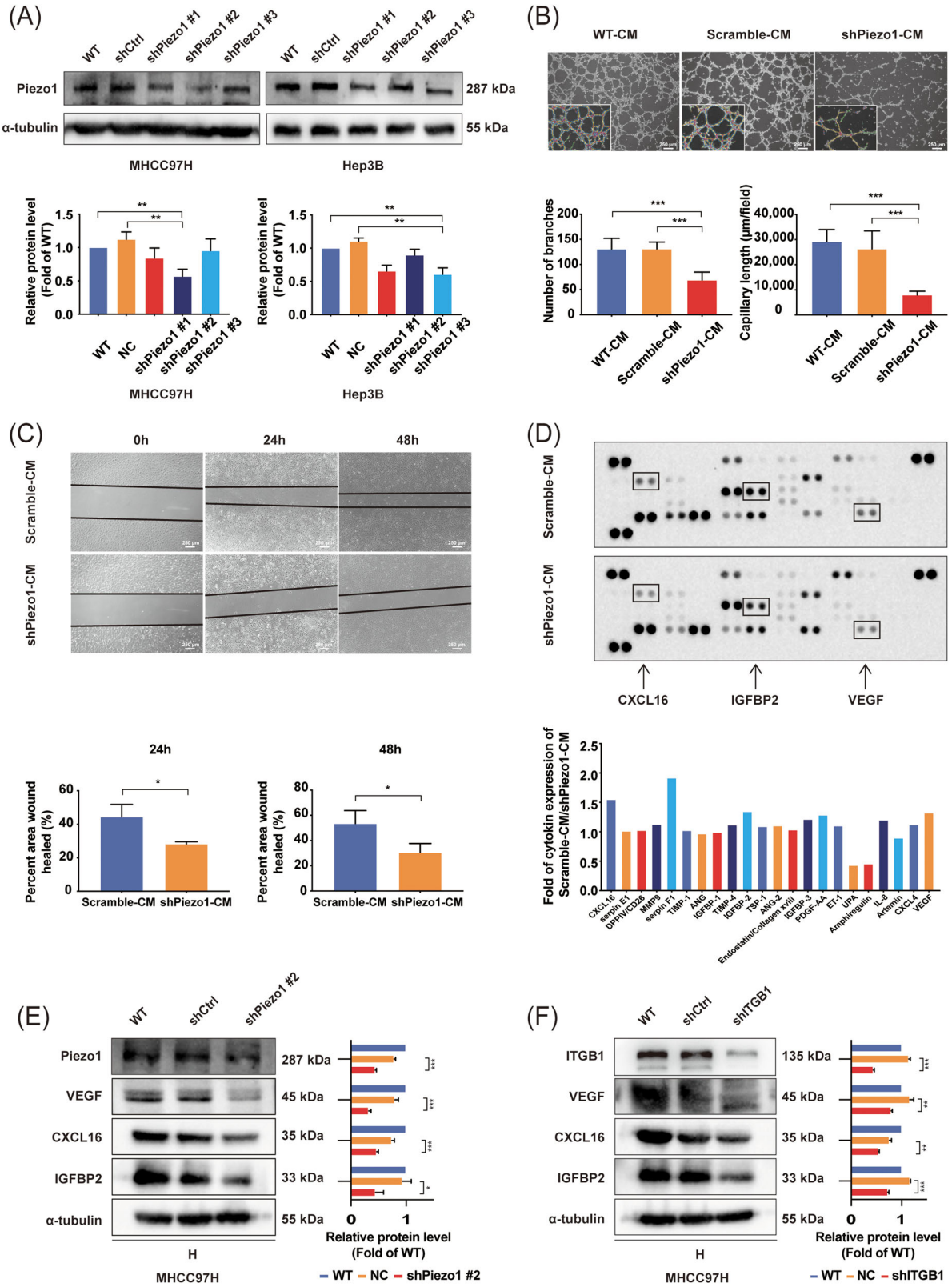

FIGURE 4 Analysis of differentially expressed pro-angiogenic and anti-angiogenic factors between shPiezo1-CM and Scramble-CM. (A) Piezo1-knockdown human HCC cell lines were verified by Western blotting. (B) Representative images of tube formation assay showed the effect of shPiezo1-CM on HUVEC tube formation. (C) Representative images of wound healing assay showed the effect of shPiezo1-CM on HUVEC migration. (D) Screening of differentially expressed pro-angiogenic and anti-angiogenic factors using a human angiogenesis array between Scramble-CM and shPiezo1-CM (upper panel). Fold change analysis of differentially expressed pro-angiogenic and anti-angiogenic factors between Scramble-CM and shPiezo1-CM (bottom panel). (E) Western blotting assay of three differentially expressed pro-angiogenic

substrate and found that MG132 intervention obviously increased the expression of HIF-1α and its downstream target genes VEGF, IGFBP2, and CXCL16 (Figure 6B and Supplementary Figure S4C-D), indirectly indicating that increased matrix stiffness repressed HIF-1α ubiquitination and promoted the expression of its downstream target genes. Afterwards, we evaluated the effects of Piezo1 activation on HIF-1α ubiquitination and the expression of its downstream target genes. The results demonstrated that Yoda1 intervention resulted in a significant upregulation in HIF-1α, VEGF, CXCL16, and IGFBP2 expression, as well as an obvious downregulation in VHL expression in HCC cells cultured on low-stiffness substrate (Figure 6C and Supplementary Figure S4E-F). GsMTx4 intervention achieved an opposite result in HCC cells cultured on high-stiffness substrate (Figure 6D, Supplementary Figure S4G-H). These results together with the data in Figure 5 suggested that Piezo1 activation inhibited HIF-1α ubiquitination and upregulated the expression of its downstream target genes via Ca^{2+} influx. Besides, Piezo1 or integrin β1 knockdown also led to a significant decline in HIF-1α, VEGF, IGFBP2, and CXCL16 expression and an increase in VHL expression in HCC cells cultured on high-stiffness substrate (Figure 6E-F and Supplementary Figure S4I-L), but Yoda1 intervention partially reversed the effects of Piezo1 or integrin β1 knockdown on the expression of HIF-1α, VHL, VEGF, IGFBP2, and CXCL16. Similarly, MG132 intervention also reversed Piezo1 downregulation-caused changes in the expression of HIF-1 and its downstream target proteins (Figure 6E-F and Supplementary Figure S4I-L). Thereby, matrix stiffness-caused Piezo1 activation participates in HIF-1α ubiquitination and the expression of its downstream pro-angiogenic factors.

Taking HIF-1α as a bait protein to capture VHL protein, we observed an endogenous interaction between VHL protein and HIF-1α protein in HCC cells (Figure 6G, Supplementary Figure S5A). Additionally, knockdown of Piezo1 or integrin β1 elevated the HIF-1α ubiquitination level (Figure 6H and Supplementary Figure S5B-C), showing direct evidence that Piezo1 participates in high matrix stiffness-downregulated HIF-1α ubiquitination. In SD rat model with high-stiffness background, the positive expression areas of HIF-1α, VEGF, CXCL16 and IGFBP2 were significantly decreased in HCC tissues of the shPiezo1 group and the shITGB1 group (Figure 6I and Supplementary Figure S5D). Moreover, the positive expression areas of HIF-1α and VEGF were associated with Piezo1-positive expression areas in human HCC tissues (Supplementary Figure S5E), validating that Piezo1 contributes to matrix stiffness-mediated effect on HIF-1α expression and angiogenesis in HCC.

Above all, we concluded that the matrix stiffness/integrin β1/Piezo1 activation/Ca^{2+} influx/HIF-1α ubiquitination/VEGF, CXCL16 and IGFBP2 pathway participates in matrix stiffness-regulated HCC angiogenesis (Figure 7).

4 | DISCUSSION

Our previous works have validated a positive correlation between stiffness mechanical signal and HCC angiogenesis [31, 32]. In the present study, we found that increased matrix stiffness significantly upregulated Piezo1 expression at both cellular and tissue levels. High expression of Piezo1 was associated with HCC angiogenesis and indicated an unfavorable prognosis. Additionally, increased matrix stiffness also noticeably enhanced Piezo1 activation and promoted Ca^{2+} influx. Under the same stiffness stimulation, the expression level of Piezo1 was consistent with its activation level. Based on the above evidence, we speculated that Piezo1 and Piezo1 activation might be required for matrix stiffness-induced angiogenesis and metastasis in HCC.

We first developed two types of animal models to validate the role of Piezo1 in matrix stiffness-induced angiogenesis and metastasis in vivo. In orthotopic liver cancer SD rat models with high liver stiffness background, knockdown of Piezo1 or integrin β1 significantly suppressed tumor growth, angiogenesis, and lung metastasis. However, in orthotopic liver cancer SD rat models with normal liver stiffness backgrounds, suppression of Piezo1 or integrin β1 only inhibited tumor growth significantly. By comparing the experimental results of two animal models, it is not difficult to conclude that high matrix stiffness promotes angiogenesis and metastasis of HCC and that Piezo1 is dispensable in matrix stiffness-mediated effects on angiogenesis and metastasis.

factors (VEGF, IGFBP2, CXCL16) in wild-type, shCtrl-transfected, and shPiezo1-transfected MHCC97H cells cultured on high-stiffness substrate. (F) Western blotting assay of VEGF, IGFBP2 and CXCL16 in wild-type, shCtrl-transfected, and shITGB1-transfected MHCC97H cells grown on high-stiffness substrate. The protein expression, number of branches, capillary length, and wound-healed area were quantified using ImageJ software. *$P < 0.05$, ** $P < 0.01$, ***$P < 0.001$.

Abbreviations: HCC, hepatocellular carcinoma; WT, wild type; Ctrl, control; CM, conditioned medium; HUVEC, human vascular endothelial; VEGF, vascular endothelial growth factor; IGFBP2, insulin like growth factor binding proteins; CXCL16, CXC chemokine ligand 16; H, high stiffness (16 kPa); ITGB1, integrin β1.

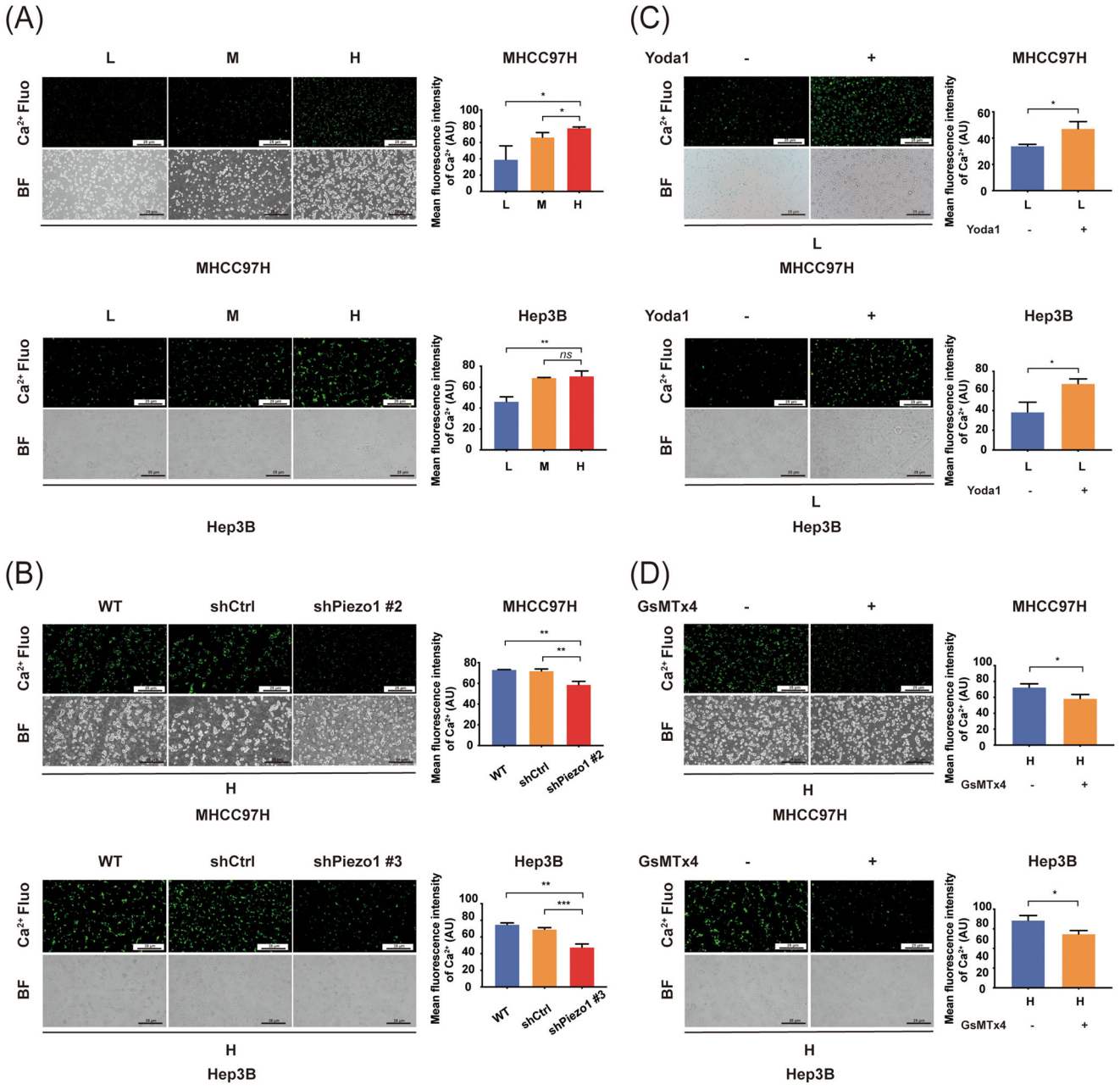

FIGURE 5 Piezo1 activation and Ca^{2+} influx in HCC cells under different stiffness stimulations. (A) Fluorescence assay to determine the intracellular Ca^{2+} in MHCC97H and Hep3B cells under different stiffness stimulations. (B) Piezo1 knockdown diminished the fluorescence intensity of intracellular Ca^{2+} in MHCC97H and Hep3B cells cultured on high-stiffness substrate. (C) Activator Yoda1 upregulated the fluorescence intensity of intracellular Ca^{2+} in MHCC97H and Hep3B cells grown on low-stiffness substrate. (D) Antagonist GsMTx4 decreased the fluorescence intensity of intracellular Ca^{2+} in MHCC97H and Hep3B cells grown on high-stiffness substrate. The fluorescence intensity of intracellular Ca^{2+} was quantified using ImageJ software. *ns*, not significant, $^{*}P < 0.05$, $^{**}P < 0.01$, $^{***}P < 0.001$. Abbreviations: HCC, hepatocellular carcinoma; L, low stiffness (6 kPa); M, medium stiffness (10 kPa); H, high stiffness (16 kPa); WT, wild type; Ctrl, control; fluo, fluorescence; BF, bright field.

On the other hand, shPiezo1-CM collected from HCC cells under high-stiffness stimulation also remarkably attenuated tube formation and migration abilities of HUVECs, indicating that Piezo1 upregulation under high-stiffness stimulation increases the expression and secretion of pro-angiogenic factors. Similarly, analysis of differentially expressed pro-angiogenic factors between shPiezo1-CM and Scramble-CM also revealed that Piezo1 promoted the expression and secretion of pro-angiogenic factors. All evidence supports that Piezo1 upregulation

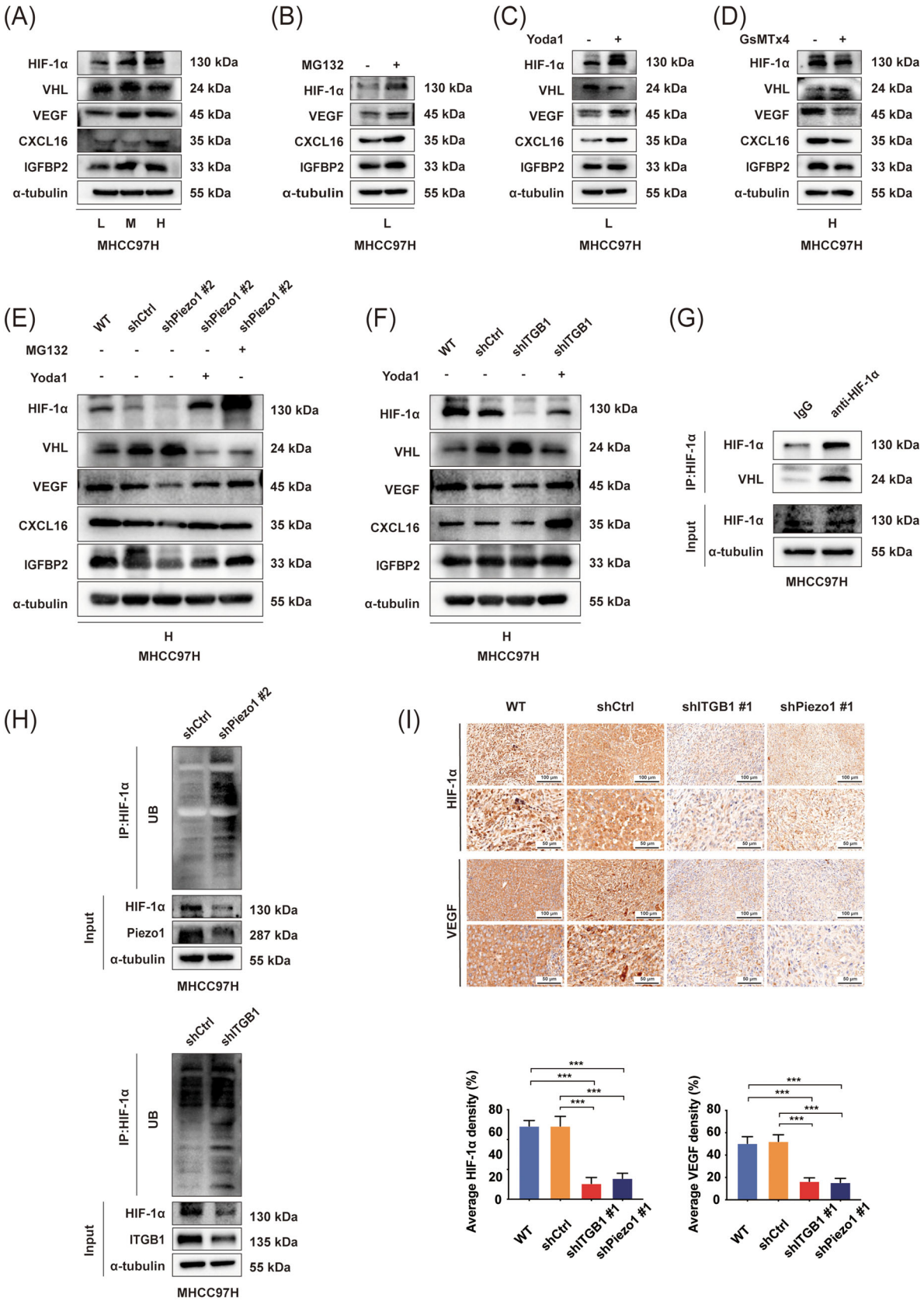

FIGURE 6 Piezo1 activation induced by high-stiffness stimulation regulates the expression of HIF-1α ubiquitination and its downstream pro-angiogenic factors in HCC cells. (A) The expression of HIF-1α, VHL, VEGF, IGFBP2 and CXCL16 in MHCC97H cells grown on different stiffness substrates. (B) MG132 intervention increased the expression of HIF-1α and its downstream target genes in MHCC97H cells cultured on low-stiffness substrate. (C) Effects of Yoda1 on the expression of HIF-1α, VHL, VEGF, IGFBP2 and CXCL16 in MHCC97H

participates in matrix stiffness-induced angiogenesis by regulating the expression of angiogenesis-related cytokines. Considering that the identified differentially expressed pro-angiogenic factors VEGF, IGFBP2 and CXCL16 have a common transcription factor, HIF-1α [16, 55, 60, 61], we determined them as the target proteins for subsequent mechanism analysis. Because Piezo1 expression and its activation exhibited the same increasing trend in HCC cells with an increase in matrix stiffness, we continued to investigate whether Piezo1 activation influenced the expression of HIF-1α and its downstream angiogenesis-related factors. Yoda1 intervention significantly reversed the downregulation of HIF-1α and its downstream angiogenesis-related factors caused by Piezo1 or integrin β1 knockdown, confirming the regulatory roles of Piezo1 activation and Ca^{2+} influx in the expression of HIF-1α and its downstream angiogenesis-related factors.

Changes in intracellular Ca^{2+} concentration can drive many pathological molecule events such as migration, invasion, proliferation and apoptosis [62–64]. Calcium channels and pumps were demonstrated to influence HIF-1 transcription, translation, stabilization and nuclear translocation in diverse types of cancer [65]. In prostate cancer cells, transient receptor potential channel M8 (TRPM8) overexpression reduced the phosphorylation level of the receptor of activated C kinase 1 (RACK1) and hindered its dimerization, and then promoted RACK1 binding to HIF-1α and calcineurin, ultimately resulted in

cells grown on low-stiffness substrate. (D) Effects of GsMTx4 on the expression of HIF-1α, VHL, VEGF, IGFBP2 and CXCL16 in MHCC97H cells grown on high-stiffness substrate. (E) Effects of Piezo1 knockdown, Yoda1 intervention and MG132 intervention on the expression of target proteins in MHCC97H cells grown on high-stiffness substrate. (F) Effects of integrin β1 knockdown and Yoda1 intervention on the expression of target proteins in HCC cells grown on high-stiffness substrate. (G) Co-IP assay demonstrates an endogenous interaction between VHL protein and HIF-1α protein. (H) HIF-1α ubiquitination level was increased in shPiezo1- or shITGB1-transfected MHCC97H cells compared with that in shCtrl-transfected MHCC97H cells. (I) Representative IHC staining images of HIF-1α and VEGF in orthotopic HCC tumors in WT, shCtrl, shITGB1 #1 and shPiezo1 #1 groups with high liver stiffness background. The protein expression area was quantified using ImageJ software. $^{***}P < 0.001$.

Abbreviations: L, low stiffness (6 kPa); M, medium stiffness (10 kPa); H, high stiffness (16 kPa); HIF-1α, hypoxia-inducible factor 1α; VEGF, vascular endothelial growth factor; IGFBP2, insulin like growth factor binding proteins; CXCL16, CXC chemokine ligand 16; VHL, von hippel-lindau; WT, wild type; Ctrl, control; ITGB1, integrin β1; IHC, immunohistochemical; Co-IP, co-immunoprecipitation.

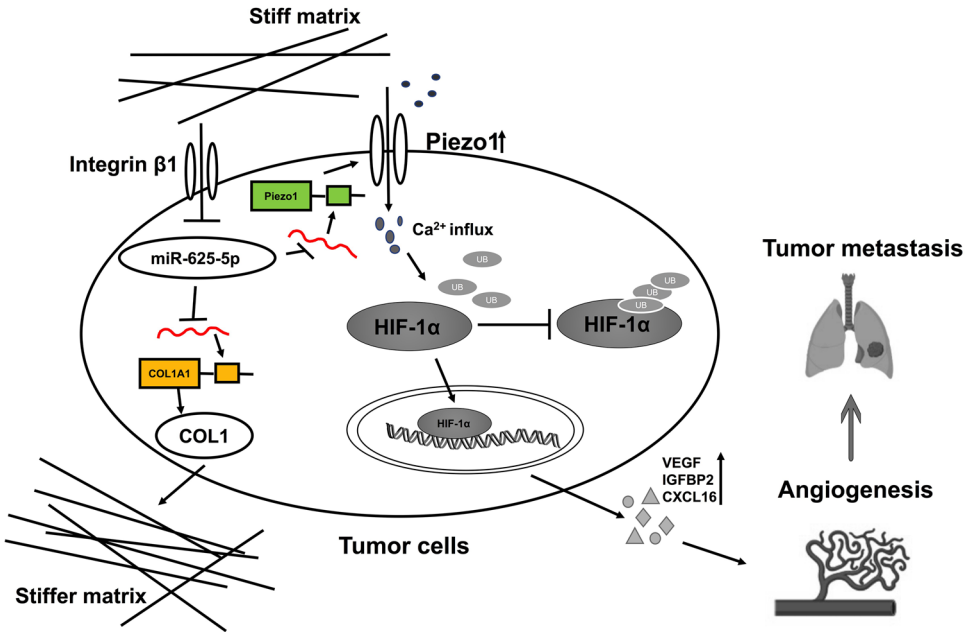

FIGURE 7 The mechanism by which activation of Piezo1 contributes to matrix stiffness-induced angiogenesis in HCC. Matrix stiffness, as an initiator, enhances Piezo1 activation and Ca^{2+} influx, and then suppresses HIF-1α ubiquitination, ultimately promoting pro-angiogenic factor expression to accelerate HCC angiogenesis. Besides, a positive feedback regulation loop as stiff matrix/integrin β1/miR-625-5p /Piezo1 and COL1/stiffer matrix mediates matrix stiffness-caused Piezo1 upregulation.

Abbreviations: HIF-1α, hypoxia-inducible factor 1α; VEGF, vascular endothelial growth factor; IGFBP2, insulin like growth factor binding proteins; CXCL16, CXC chemokine ligand 16; COL1, collagen1; UB, ubiquitin.

a decrease in HIF-1α ubiquitination [66]. In neuroblastoma cells, full-length transient receptor potential channel M2 decreased the expression of VHL to impede HIF-1α degradation [67]. Based on an obvious downregulation in VHL in HCC cells under high-stiffness stimulation and an increase in the expression of HIF-1α and its downstream target genes under MG132 intervention, we further conjectured that increased matrix stiffness might repress HIF-1α ubiquitination and promote the expression of its downstream target genes through Piezo1 activation. Yoda1 or GsMTx4 intervention assay under low- or high-stiffness stimulation all supported that Piezo1 activation inhibited HIF-1α ubiquitination and upregulated the expression of its downstream target genes. Co-IP assay also revealed an endogenous interaction between VHL protein and HIF-1α protein and that shPiezo1- or shITGB1-transfected HCC cells had an obvious increase in HIF-1α ubiquitination level, giving direct evidence that Piezo1 participates in high matrix stiffness-downregulated HIF-1α ubiquitination. Taken together, matrix stiffness as an initiator enhanced Piezo1 activation and Ca^{2+} influx, and then suppressed HIF-1α ubiquitination, ultimately promoting pro-angiogenic factor expression to accelerate HCC angiogenesis.

In addition to upregulating Piezo1 expression, increased matrix stiffness also significantly improved COL1 expression in HCC cells. In view of the dominant role of matrix protein deposition and crosslinking in matrix stiffening [41], we proposed a hypothesis that COL1-reinforced tissue stiffening may result in upregulated expression of Piezo1. Our results showed that the increase of COL1 deposition evidently raised the stiffness of the surrounding matrix and caused the appearance of thick bundle collagen, confirming the hypothesis that COL1 deposition reinforced tissue stiffening. Given that a miRNA can simultaneously regulate the expression of multiple target proteins [68], we identified miR-625-5p as a common miRNA to analyze its effects on Piezo1 and COL1A1. Under the same stiffness stimulation, the expression of miR-625-5p in HCC cells was associated with the expression of Piezo1 and COL1A1. Additionally, increased matrix stiffness significantly downregulated miR-625-5p expression, while the suppression of integrin β1 reversed high stiffness-induced miR-625-5p downregulation. Dual-luciferase reporter assay revealed a specific binding between miR-625-5p and the 3'-UTR sites of Piezo1 or COL1A1. Analysis of miR-625-5p overexpression or downregulation also supported that miR-625-5p mediated matrix stiffness-caused Piezo1 and COL1A1 upregulation. In summary, a positive feedback regulation loop as stiff matrix/integrin β1/miR-625-5p/Piezo1 and COL1/stiffer matrix was involved in matrix stiffness-upregulated Piezo1 expression.

Because the obtained evidence supports that increased matrix stiffness can enhance the release and expression of multiple pro-angiogenic factors to accelerate HCC angiogenesis, we think that targeting the anti-angiogenic effect of initiating factor matrix stiffness may be superior to that of specific angiogenic factors such as VEGF. Additionally, Piezo1 serves as an upstream molecule in mechanosensory pathway to mediate matrix stiffness-induced angiogenesis and indicates a worse prognosis in HCC, which means that Piezo1 may become a promising novel target in anti-angiogenic therapy. Nonetheless, it should be mentioned that there were several limitations in the present study. Although the stiffness-sensor molecule integrin β1 was validated to regulate the expression and activity of Piezo1, the direct effect of mechanical signal on Piezo1 activation could not be excluded. Whether there exists a Piezo1-based mechanosensory pathway independent of integrin β1 merits to be further investigated in further research. Besides, the detailed mechanism about how elevated Ca^{2+} influx influences HIF-1α ubiquitination could be addressed in the follow-up study.

5 | CONCLUSIONS

Our study unravels a new mechanism by which integrin β1/Piezo1 activation/Ca^{2+} influx/HIF-1α ubiquitination/VEGF, CXCL16 and IGFBP2 pathway participates in matrix stiffness-driven HCC angiogenesis. Simultaneously, a positive feedback regulation loop as stiff matrix/integrin β1/miR-625-5p /Piezo1 and COL1/stiffer matrix mediates matrix stiffness-caused Piezo1 upregulation.

AUTHOR CONTRIBUTIONS

All authors contributed to the study conception and design. Jiefeng Cui and Zhenggang Ren proposed conceptualizations and designed the study. Miao Li, Xi Zhang, Mimi Wang, Jiali Qian, Xiaoxia Xing, Yaohui Wang and Yang You developed the experiment methods and completed all the experiments. Jie Chen, Dongmei Gao and Yan Zhao helped finish the animal experiment. Zhiming Wang, Kun Guo, Lan Zhang and Rongxin Chen provided guidance and suggestion for the experiments. Miao Li and Xi Zhang wrote the original draft, and Jiefeng Cui and Zhenggang Ren revised it. All the authors read and approved the final manuscript.

ACKNOWLEDGMENTS

The present study was supported by a grant from the National Natural Science Foundation of China (Grant No. 81972910).

COMPETING INTERESTS

The authors declare that they have no competing interests.

DATA AVAILABILITY STATEMENT

The data that support the findings of this study are available from the corresponding author upon reasonable request.

ETHICS APPROVAL AND CONSENT TO PARTICIPATE

Human HCC tissues and clinical data used in the study were approved by the Zhongshan Hospital Research Ethics Committee (Approval No. B2019-332R). All animal experiments were approved by the Animal Care Ethical Committee of Zhongshan Hospital (Approval No. 2019-136).

CONSENT FOR PUBLICATION

Not applicable.

ORCID

Miao Li https://orcid.org/0000-0001-7840-7511

REFERENCES

1. Fidler IJ. Angiogenesis and cancer metastasis. Cancer J. 2000;6 Suppl 2:S134-41.
2. Ribatti D, Vacca A, Nico B, Sansonno D, Dammacco F. Angiogenesis and anti-angiogenesis in hepatocellular carcinoma. Cancer Treat Rev. 2006;32(6):437-44.
3. Pang R, Poon RT. Angiogenesis and antiangiogenic therapy in hepatocellular carcinoma. Cancer Lett. 2006;242(2):151-67.
4. Wang YH, Dong YY, Wang WM, Xie XY, Wang ZM, Chen RX, et al. Vascular endothelial cells facilitated HCC invasion and metastasis through the Akt and NF-κB pathways induced by paracrine cytokines. J Exp Clin Cancer Res. 2013;32(1):51.
5. Teleanu RI, Chircov C, Grumezescu AM, Teleanu DM. Tumor Angiogenesis and Anti-Angiogenic Strategies for Cancer Treatment. J Clin Med. 2019;9(1):84.
6. Rizzo A, Dadduzio V, Ricci AD, Massari F, Di Federico A, Gadaleta-Caldarola G, et al. Lenvatinib plus pembrolizumab: the next frontier for the treatment of hepatocellular carcinoma? Expert Opin Investig Drugs. 2022;31(4):371-8.
7. Yang JD, Hainaut P, Gores GJ, Amadou A, Plymoth A, Roberts LR. A global view of hepatocellular carcinoma: trends, risk, prevention and management. Nat Rev Gastroenterol Hepatol. 2019;16(10):589-604.
8. Llovet JM, Montal R, Sia D, Finn RS. Molecular therapies and precision medicine for hepatocellular carcinoma. Nat Rev Clin Oncol. 2018;15(10):599-616.
9. Huang A, Yang XR, Chung WY, Dennison AR, Zhou J. Targeted therapy for hepatocellular carcinoma. Signal Transduct Target Ther. 2020;5(1):146.
10. Morse MA, Sun W, Kim R, He AR, Abada PB, Mynderse M, et al. The Role of Angiogenesis in Hepatocellular Carcinoma. Clin Cancer Res. 2019;25(3):912-20.
11. Wang Z, Dabrosin C, Yin X, Fuster MM, Arreola A, Rathmell WK, et al. Broad targeting of angiogenesis for cancer prevention and therapy. Semin Cancer Biol. 2015;35(Suppl):S224-s43.
12. Rizzo A, Brandi G. Biochemical predictors of response to immune checkpoint inhibitors in unresectable hepatocellular carcinoma. Cancer Treat Res Commun. 2021;27:100328.
13. Farnsworth RH, Lackmann M, Achen MG, Stacker SA. Vascular remodeling in cancer. Oncogene. 2014;33(27):3496-505.
14. Gupta MK, Qin RY. Mechanism and its regulation of tumor-induced angiogenesis. World J Gastroenterol. 2003;9(6):1144-55.
15. Krock BL, Skuli N, Simon MC. Hypoxia-induced angiogenesis: good and evil. Genes Cancer. 2011;2(12):1117-33.
16. Semenza GL. Hypoxia-inducible factors: mediators of cancer progression and targets for cancer therapy. Trends Pharmacol Sci. 2012;33(4):207-14.
17. Schrader J, Gordon-Walker TT, Aucott RL, van Deemter M, Quaas A, Walsh S, et al. Matrix stiffness modulates proliferation, chemotherapeutic response, and dormancy in hepatocellular carcinoma cells. Hepatology. 2011;53(4):1192-205.
18. Dong Y, Zheng Q, Wang Z, Lin X, You Y, Wu S, et al. Higher matrix stiffness as an independent initiator triggers epithelial-mesenchymal transition and facilitates HCC metastasis. J Hematol Oncol. 2019;12(1):112.
19. Tang RZ, Gu SS, Chen XT, He LJ, Wang KP, Liu XQ. Immobilized Transforming Growth Factor-Beta 1 in a Stiffness-Tunable Artificial Extracellular Matrix Enhances Mechanotransduction in the Epithelial Mesenchymal Transition of Hepatocellular Carcinoma. ACS Appl Mater Interfaces. 2019;11(16):14660-71.
20. Wu S, Zheng Q, Xing X, Dong Y, Wang Y, You Y, et al. Matrix stiffness-upregulated LOXL2 promotes fibronectin production, MMP9 and CXCL12 expression and BMDCs recruitment to assist pre-metastatic niche formation. J Exp Clin Cancer Res. 2018;37(1):99.
21. Wu S, Xing X, Wang Y, Zhang X, Li M, Wang M, et al. The pathological significance of LOXL2 in pre-metastatic niche formation of HCC and its related molecular mechanism. Eur J Cancer. 2021;147:63-73.
22. You Y, Zheng Q, Dong Y, Xie X, Wang Y, Wu S, et al. Matrix stiffness-mediated effects on stemness characteristics occurring in HCC cells. Oncotarget. 2016;7(22):32221-31.
23. Zhao W, Lv M, Yang X, Zhou J, Xing B, Zhang Z. Liver tumor-initiating cells initiate the formation of a stiff cancer stem cell microenvironment niche by secreting LOX. Carcinogenesis. 2022 Apr 18:bgac035.
24. You Y, Zheng Q, Dong Y, Wang Y, Zhang L, Xue T, et al. Higher Matrix Stiffness Upregulates Osteopontin Expression in Hepatocellular Carcinoma Cells Mediated by Integrin β1/GSK3β/β-Catenin Signaling Pathway. PLoS One. 2015;10(8):e0134243.
25. Yang N, Chen T, Wang L, Liu R, Niu Y, Sun L, et al. CXCR4 mediates matrix stiffness-induced downregulation of UBTD1 driving hepatocellular carcinoma progression via YAP signaling pathway. Theranostics. 2020;10(13):5790-801.
26. Liu HH, Xu Y, Li CJ, Hsu SJ, Lin XH, Zhang R, et al. An SCD1-dependent mechanoresponsive pathway promotes HCC invasion and metastasis through lipid metabolic reprogramming. Mol Ther. 2022;30(7):2554-67.
27. Liu QP, Luo Q, Deng B, Ju Y, Song GB. Stiffer Matrix Accelerates Migration of Hepatocellular Carcinoma Cells through

Enhanced Aerobic Glycolysis Via the MAPK-YAP Signaling. Cancers (Basel). 2020;12(2).
28. Filliol A, Schwabe RF. Contributions of Fibroblasts, Extracellular Matrix, Stiffness, and Mechanosensing to Hepatocarcinogenesis. Semin Liver Dis. 2019;39(3):315-33.
29. Liu QP, Luo Q, Deng B, Ju Y, Song GB. Stiffer Matrix Accelerates Migration of Hepatocellular Carcinoma Cells through Enhanced Aerobic Glycolysis Via the MAPK-YAP Signaling. Cancers (Basel). 2020;12(2):490.
30. Gao X, Qiao X, Xing X, Huang J, Qian J, Wang Y, et al. Matrix Stiffness-Upregulated MicroRNA-17-5p Attenuates the Intervention Effects of Metformin on HCC Invasion and Metastasis by Targeting the PTEN/PI3K/Akt Pathway. Front Oncol. 2020;10:1563.
31. Dong Y, Xie X, Wang Z, Hu C, Zheng Q, Wang Y, et al. Increasing matrix stiffness upregulates vascular endothelial growth factor expression in hepatocellular carcinoma cells mediated by integrin β1. Biochem Biophys Res Commun. 2014;444(3):427-32.
32. Wang Y, Zhang X, Wang W, Xing X, Wu S, Dong Y, et al. Integrin αVβ5/Akt/Sp1 pathway participates in matrix stiffness-mediated effects on VEGFR2 upregulation in vascular endothelial cells. Am J Cancer Res. 2020;10(8):2635-48.
33. Levental KR, Yu H, Kass L, Lakins JN, Egeblad M, Erler JT, et al. Matrix crosslinking forces tumor progression by enhancing integrin signaling. Cell. 2009;139(5):891-906.
34. Wu J, Lewis AH, Grandl J. Touch, Tension, and Transduction - The Function and Regulation of Piezo Ion Channels. Trends Biochem Sci. 2017;42(1):57-71.
35. Yang XN, Lu YP, Liu JJ, Huang JK, Liu YP, Xiao CX, et al. Piezo1 is as a novel trefoil factor family 1 binding protein that promotes gastric cancer cell mobility in vitro. Dig Dis Sci. 2014;59(7):1428-35.
36. Tsuchiya M, Hara Y, Okuda M, Itoh K, Nishioka R, Shiomi A, et al. Cell surface flip-flop of phosphatidylserine is critical for PIEZO1-mediated myotube formation. Nat Commun. 2018;9(1):2049.
37. Lin YC, Guo YR, Miyagi A, Levring J, MacKinnon R, Scheuring S. Force-induced conformational changes in PIEZO1. Nature. 2019;573(7773):230-4.
38. Chen X, Wanggou S, Bodalia A, Zhu M, Dong W, Fan JJ, et al. A Feedforward Mechanism Mediated by Mechanosensitive Ion Channel PIEZO1 and Tissue Mechanics Promotes Glioma Aggression. Neuron. 2018;100(4):799-815.e7.
39. Kang H, Hong Z, Zhong M, Klomp J, Bayless KJ, Mehta D, et al. Piezo1 mediates angiogenesis through activation of MT1-MMP signaling. Am J Physiol Cell Physiol. 2019;316(1):C92-c103.
40. Wang TH, Hsia SM, Shieh TM. Lysyl Oxidase and the Tumor Microenvironment. Int J Mol Sci. 2016;18(1).
41. Xu S, Xu H, Wang W, Li S, Li H, Li T, et al. The role of collagen in cancer: from bench to bedside. J Transl Med. 2019;17(1):309.
42. Marrero JA, Kulik LM, Sirlin CB, Zhu AX, Finn RS, Abecassis MM, et al. Diagnosis, Staging, and Management of Hepatocellular Carcinoma: 2018 Practice Guidance by the American Association for the Study of Liver Diseases. Hepatology. 2018;68(2):723-50.
43. Llovet JM, Fuster J, Bruix J. The Barcelona approach: diagnosis, staging, and treatment of hepatocellular carcinoma. Liver Transpl. 2004;10(2 Suppl 1):S115-20.
44. Amin MB, Greene FL, Edge SB, Compton CC, Gershenwald JE, Brookland RK, et al. The Eighth Edition AJCC Cancer Staging Manual: Continuing to build a bridge from a population-based to a more "personalized" approach to cancer staging. CA Cancer J Clin. 2017;67(2):93-9.
45. Edmondson HA, Steiner PE. Primary carcinoma of the liver: a study of 100 cases among 48,900 necropsies. Cancer. 1954;7(3):462-503.
46. Agbim U, Asrani SK. Non-invasive assessment of liver fibrosis and prognosis: an update on serum and elastography markers. Expert Rev Gastroenterol Hepatol. 2019;13(4):361-74.
47. Terada H, Komeichi H, Aramaki T. [Child-Pugh classification in liver cirrhosis]. Ryoikibetsu Shokogun Shirizu. 1995(7):151-4.
48. Bedossa P, Poynard T. An algorithm for the grading of activity in chronic hepatitis C. The METAVIR Cooperative Study Group. Hepatology. 1996;24(2):289-93.
49. EASL-ALEH Clinical Practice Guidelines: Non-invasive tests for evaluation of liver disease severity and prognosis. J Hepatol. 2015;63(1):237-64.
50. Sullivan R, Maresh G, Zhang X, Salomon C, Hooper J, Margolin D, et al. The Emerging Roles of Extracellular Vesicles As Communication Vehicles within the Tumor Microenvironment and Beyond. Front Endocrinol (Lausanne). 2017;8:194.
51. Naito Y, Yoshioka Y, Yamamoto Y, Ochiya T. How cancer cells dictate their microenvironment: present roles of extracellular vesicles. Cell Mol Life Sci. 2017;74(4):697-713.
52. Maacha S, Bhat AA, Jimenez L, Raza A, Haris M, Uddin S, et al. Extracellular vesicles-mediated intercellular communication: roles in the tumor microenvironment and anti-cancer drug resistance. Mol Cancer. 2019;18(1):55.
53. Wang JC, Li GY, Li PP, Sun X, Li WM, Li Y, et al. Suppression of hypoxia-induced excessive angiogenesis by metformin via elevating tumor blood perfusion. Oncotarget. 2017;8(43):73892-904.
54. Luo W, Hu H, Chang R, Zhong J, Knabel M, O'Meally R, et al. Pyruvate kinase M2 is a PHD3-stimulated coactivator for hypoxia-inducible factor 1. Cell. 2011;145(5):732-44.
55. Gao Q, Zhao YJ, Wang XY, Qiu SJ, Shi YH, Sun J, et al. CXCR6 upregulation contributes to a proinflammatory tumor microenvironment that drives metastasis and poor patient outcomes in hepatocellular carcinoma. Cancer Res. 2012;72(14):3546-56.
56. Azar WJ, Azar SH, Higgins S, Hu JF, Hoffman AR, Newgreen DF, et al. IGFBP-2 enhances VEGF gene promoter activity and consequent promotion of angiogenesis by neuroblastoma cells. Endocrinology. 2011;152(9):3332-42.
57. Zanotelli MR, Reinhart-King CA. Mechanical Forces in Tumor Angiogenesis. Adv Exp Med Biol. 2018;1092:91-112.
58. Lee JW, Bae SH, Jeong JW, Kim SH, Kim KW. Hypoxia-inducible factor (HIF-1)alpha: its protein stability and biological functions. Exp Mol Med. 2004;36(1):1-12.
59. Xing X, Wang Y, Zhang X, Gao X, Li M, Wu S, et al. Matrix stiffness-mediated effects on macrophages polarization and their LOXL2 expression. Febs j. 2021;288(11):3465-77.
60. Choi KS, Bae MK, Jeong JW, Moon HE, Kim KW. Hypoxia-induced angiogenesis during carcinogenesis. J Biochem Mol Biol. 2003;36(1):120-7.
61. Semenza GL. Targeting HIF-1 for cancer therapy. Nat Rev Cancer. 2003;3(10):721-32.
62. Zhang J, Wei J, Kanada M, Yan L, Zhang Z, Watanabe H, et al. Inhibition of store-operated Ca2+ entry suppresses

EGF-induced migration and eliminates extravasation from vasculature in nasopharyngeal carcinoma cell. Cancer Lett. 2013;336(2):390-7.
63. Simons M, Gordon E, Claesson-Welsh L. Mechanisms and regulation of endothelial VEGF receptor signalling. Nat Rev Mol Cell Biol. 2016;17(10):611-25.
64. Han Y, Liu C, Zhang D, Men H, Huo L, Geng Q, et al. Mechanosensitive ion channel Piezo1 promotes prostate cancer development through the activation of the Akt/mTOR pathway and acceleration of cell cycle. Int J Oncol. 2019;55(3):629-44.
65. Azimi I. The interplay between HIF-1 and calcium signalling in cancer. Int J Biochem Cell Biol. 2018;97:73-7.
66. Yu S, Xu Z, Zou C, Wu D, Wang Y, Yao X, et al. Ion channel TRPM8 promotes hypoxic growth of prostate cancer cells via an O2 -independent and RACK1-mediated mechanism of HIF-1α stabilization. J Pathol. 2014;234(4):514-25.
67. Chen SJ, Hoffman NE, Shanmughapriya S, Bao L, Keefer K, Conrad K, et al. A splice variant of the human ion channel TRPM2 modulates neuroblastoma tumor growth through hypoxia-inducible factor (HIF)-1/2α. J Biol Chem. 2014;289(52):36284-302.
68. Li D, Zhang J, Li J. Role of miRNA sponges in hepatocellular carcinoma. Clin Chim Acta. 2020;500:10-9.

SUPPORTING INFORMATION

Additional supporting information can be found online in the Supporting Information section at the end of this article.

How to cite this article: Li M, Zhang X, Wang M, Wang Y, Qian J, Xing X, et al. Activation of Piezo1 contributes to matrix stiffness-induced angiogenesis in hepatocellular carcinoma. Cancer Commun. 2022;42:1162–1184.
https://doi.org/10.1002/cac2.12364